MOLECULAR AND CELLULAR BIOLOGY, Feb. 2011, p. 557–572 Vol. 31, No. 3
0270-7306/11/$12.00 doi:10.1128/MCB.00909-10

Spt10 and Swi4 Control the Timing of Histone H2A/H2B Gene Activation in Budding Yeast[▽]

Peter R. Eriksson, Dwaipayan Ganguli, and David J. Clark*

Program in Genomics of Differentiation, NICHD, National Institutes of Health, Building 6A, Room 2A14, 6 Center Drive, Bethesda, Maryland 20892-2426

Received 5 August 2010/Returned for modification 6 September 2010/Accepted 17 November 2010

The expression of the histone genes is regulated during the cell cycle to provide histones for nucleosome assembly during DNA replication. In budding yeast, histones H2A and H2B are expressed from divergent promoters at the *HTA1-HTB1* and *HTA2-HTB2* loci. Here, we show that the major activator of *HTA1-HTB1* is Spt10, a sequence-specific DNA binding protein with a putative histone acetyltransferase (HAT) domain. Spt10 binds to two pairs of upstream activation sequence (UAS) elements in the *HTA1-HTB1* promoter: UAS1 and UAS2 drive *HTA1* expression, and UAS3 and UAS4 drive *HTB1* expression. UAS3 and UAS4 also contain binding sites for the cell cycle regulator SBF (an Swi4-Swi6 heterodimer), which overlap the Spt10 binding sites. The binding of Spt10 and binding of SBF to UAS3 and UAS4 are mutually exclusive *in vitro*. Both SBF and Spt10 are bound in cells arrested with α-factor, apparently awaiting a signal to activate transcription. Soon after the removal of α-factor, SBF initiates a small, early peak of *HTA1* and *HTB1* transcription, which is followed by a much larger peak due to Spt10. Both activators dissociate from the *HTA1-HTB1* promoter after expression has been activated. Thus, SBF and Spt10 cooperate to control the timing of *HTA1-HTB1* expression.

The basic structural unit of chromatin is the nucleosome, which is composed of two molecules each of the four core histones, H2A, H2B, H3, and H4, formed into an octamer, around which is wrapped ~147 bp of DNA in 1.75 superhelical turns (34). Nucleosomes are formed into regularly spaced arrays along the DNA and can be mobilized by various ATP-dependent remodeling machines, such as SWI/SNF and RSC. The histones are subject to numerous posttranslational modifications, including acetylation and methylation (65). Chromatin structure plays a central role in gene regulation and other nuclear processes, including DNA replication (23). In the latter case, the cell must replicate not only its DNA during S phase but also its chromatin. Consequently, the histone genes are activated at the beginning of S phase to provide sufficient core histones to assemble all of the replicated DNA into chromatin. The inhibition of DNA synthesis results in a rapid repression of the histone genes, indicating that it is tightly coupled to DNA replication (48). Some histone gene expression is independent of replication, providing histones for chromatin assembly occurring outside S phase (61). In general, though, the regulation of the histone genes is an important aspect of eukaryotic cell cycle control (4).

The major core histone genes of the yeast *Saccharomyces cerevisiae* are organized into four loci, each containing two histone genes divergently transcribed from a central promoter: two loci encode H2A and H2B (*HTA1-HTB1* and *HTA2-HTB2*) (27), and the other two loci encode H3 and H4 (*HHT1-HHF1* and *HHT2-HHF2*) (57). The regulation of the yeast histone genes has been studied extensively (24, 48). Our focus is on the *HTA1-HTB1* locus, in which several elements that are important for cell cycle-dependent regulation have been identified.

First, there are four upstream activation sequences (UASs) (histone UAS elements), which direct correct cell cycle regulation when transposed onto a heterologous promoter (49). Histone UAS elements are found in all of the major core histone promoters (16). We have shown that they are bound by Spt10, a sequence-specific DNA binding protein (16), which contains a histone acetyltransferase (HAT) domain (43). This HAT domain has not yet been shown to have HAT activity, but the putative catalytic residues are required for the transcriptional activation of a reporter (28). Although there is indirect evidence that Spt10 might acetylate H3-K56 at the histone gene promoters (68), it has since been shown that Rtt109 is the HAT responsible for most, if not all, H3-K56 acetylation in yeast (15, 25). Spt10 is a dimer that binds specifically to pairs of histone UAS elements, each having the bipartite sequence RTTC-N_7-TTCNC, which are found only in the histone promoters (16, 38, 39). Although *SPT10* is not an essential gene, the null mutant is very sick (14, 41, 42). It displays global changes in gene regulation, which we have attributed to a defective chromatin structure arising from insufficient histone synthesis (16).

Second, the *HTA1-HTB1* promoter contains an ~67-bp negative regulatory region, referred to as the CCR or NEG region (48). The NEG region presumably contains one or more binding sites for sequence-specific factors, but these have not yet been identified. A short consensus sequence that is present in all histone loci except *HTA2-HTB2* has been termed the NEG or NRS element (20, 35, 48). The NEG element overlaps another element, called CCR′, which has some palindromic character. CCR′ confers cell cycle-dependent expression on a heterologous promoter, although the peak is early relative to that of normal histone gene expression (49). The NEG region is required for the

* Corresponding author. Mailing address: Program in Genomics of Differentiation, NICHD, National Institutes of Health, Building 6A, Room 2A14, 6 Center Drive, Bethesda, MD 20892-2426. Phone: (301) 496-6966. Fax: (301) 480-1907. E-mail: clarkda@mail.nih.gov.

▽ Published ahead of print on 29 November 2010.

rapid shutdown of histone gene transcription that occurs when cells are treated with hydroxyurea to inhibit DNA replication. This shutdown is dependent on the HIR complex (54, 58, 67), which contains Hir1, Hir2, Hir3, and Hpc2 (22, 51). The HIR complex has additional functions in transcript elongation (19, 46) and silencing (53), probably involving its histone chaperone activity (22). The NEG region is required for the recruitment of the histone chaperones Asf1 (59) and Rtt106 (18), the SWI/SNF complex (11), and the RSC complex (44). In addition, the NEG region and the HIR complex are required to mediate a compensatory response to variations in copy number of *HTA1-HTB1* (40). Thus, the NEG region plays a major role in the cell cycle control of *HTA1-HTB1*. However, it is important to note that multiple copies of UAS elements from *HTA1-HTB1* or from *HHT1-HHF1* are by themselves sufficient to direct correct cell cycle activation (20, 48, 49).

Third, the 3′-untranslated region (UTR) of *HTB1*, when attached to a reporter gene, also directs cell cycle-dependent expression, although the peak is slightly later than the peak of endogenous *HTB1* expression (7, 66).

Another sequence-specific protein with a role in *HTA1-HTB1* regulation is the SBF transcription factor, a well-studied regulator of G_1/S-specific genes (5, 6, 12). SBF is a complex between Swi4 and Swi6 (1). The activity of Swi4, which contains the DNA binding domain (DBD) (Swi4-DBD), is regulated by the cell cycle-dependent nuclear import of Swi6 (2, 55). Swi6 also binds Mbp1 to form MBF, the other major G_1/S-phase regulator in yeast. Although cells can survive without Swi4, Swi6, or Mbp1, they are rather sick, and an *swi4*Δ *mbp1*Δ double mutant is inviable (33). The evidence that SBF plays a role at *HTA1-HTB1* includes (i) genetic studies showing that both the *swi4*Δ and *mbp1*Δ mutations are synthetically lethal with the *spt10*Δ mutation (29), (ii) SBF mutants exhibiting a modest reduction in *HTA1* and *HTB1* mRNA levels (29), (iii) chromatin immunoprecipitation (ChIP) data indicating that Swi4 is present at *HTA1-HTB1* (56), and (iv) predicted SBF binding sites in the *HTA1-HTB1* promoter (discussed below). SBF activity has been correlated with the dimethylation of H3-K79, suggesting a link between this histone mark and the regulation of the G_1-to-S-phase transition (37, 52).

Here, we address the roles of Spt10 and SBF in the cell cycle-dependent regulation of *HTA1-HTB1*. We show that these proteins bind to overlapping sites within two of the four histone UAS elements in a mutually exclusive manner. Together, these two activators can account for the cell cycle dependence of *HTA1-HTB1* transcription: SBF is responsible for a small early peak of transcription, while Spt10 contributes a later, much larger peak. Although Spt10 and SBF both activate *HTA1-HTB1* expression, the difference in the timing of this activation suggests that their functions are not redundant. In their absence, there is little residual expression. We conclude that SBF and Spt10 together control the timing of *HTA1-HTB1* expression.

MATERIALS AND METHODS

All oligonucleotides used in this work are listed in Table 1.

Reporter plasmids. A reporter plasmid (p532) containing the wild-type (WT) divergent *HTA1-HTB1* promoter with the *HTA1* promoter driving RedStar-2 (RDS2) and the *HTB1* promoter driving green fluorescent protein (GFP) was constructed as follows. The *HTA1-HTB1* promoter (from start codon to start codon) was obtained as an 841-bp PstI-SpeI PCR fragment using p474 (16) as a template with primers 986 and 987, which also introduced BamHI and NheI sites, and inserted into pRS415 (Stratagene) cut with PstI and SpeI to obtain p526. The RDS2 open reading frame (ORF) was obtained by PCR as a 681-bp BamHI-PstI fragment using pYM43 (p524) (30) as a template and primers 988 and 989 and inserted at these sites into p526 to give p528. The 3′-UTR of *HTA1* was obtained as a 378-bp PstI-XhoI fragment by PCR using p474 as a template and primers 994 and 995 and inserted after the RDS2 ORF in p528 to give p529. The GFP ORF with a BglII site inserted just prior to the stop codon was obtained as a 732-bp NheI-SpeI fragment by PCR using pYM44 (p525) (30) as a template and primers 990 and 991 and inserted at these sites in p529 to yield p530. The 3′-UTR of *HTB1* was obtained as a 310-bp SpeI-NotI fragment by PCR using p474 as template with primers 992 and 993 and inserted after the GFP ORF in p530 to give p531. A 543-bp BglII fragment encoding PEST sequences from *CLN2* (36) was obtained by PCR using yeast genomic DNA as a template and primers 996 and 997 and was inserted at the BglII site at the C terminus of GFP to give p532. For reporter plasmids with mutations in both UAS1 and UAS2 (p533), the 441-bp BamHI-AfeI *HTA1* promoter fragment in p532 was replaced with a mutated version obtained by PCR using p531 as a template and primers 986 and 1010 (mutations in UAS1 are marked with a BsrGI site; those in UAS2 are marked with a PleI site). For mutations in both UAS3 and UAS4 (p541), the 829-bp BamHI-NheI *HTA1-HTB1* promoter fragment in p532 was replaced with a mutated version obtained by ligating two PCR fragments together, made using p532 as a template and primers 986 and 1035, and primers 987 and 1034 (mutations in UAS3 are marked with an AflII site; those in UAS4 are marked with a BssHII site). For all four fully mutated UAS elements (p545), the 441-bp BamHI-AfeI *HTA1* promoter fragment in p541 was replaced with a mutated version made by using primers 986 and 1010. Mutations in all four Spt10 half-sites (p598) and point mutations in the two Swi4 sites (p652) were introduced into p532 using synthesized mutated *HTA1-HTB1* promoter fragments. All inserts were sequenced.

Integration plasmids. An integration plasmid containing the wild-type *HTA1-HTB1* locus with *HIS3* inserted downstream of *HTA1* (p592) was constructed as follows. The 2,903-bp MscI-BamHI fragment from pCC67 (8), containing the *HTA1-HTB1* locus, was inserted into pNEB193 (New England Biolabs) cut with SmaI and BamHI to form p577. p592 was obtained by the insertion of a 984-bp BtgI fragment containing the *HIS3* gene (obtained by PCR using pGEM-TAHIS3 [31] as a template with primers 1151 and 1152) at the BtgI site downstream of *HTA1* in p577, such that *HIS3* and *HTA1* are transcribed in the same direction. Mutations in all four Spt10 half-sites were introduced into p592 by replacing the PflMI-EcoRV fragment with mutated versions made by PCR (p656): a megaprimer was made by using p598 as a template with primers 1292 and 1293 and then paired with primer 986; the final product was obtained by using primers 1293 and 1294. Point mutations in the two Swi4 sites were introduced into p592 in the same way, using p652 as a template, to obtain p657. Yeast was transformed with an EcoRI-BamHI digest of the integration plasmid. An integration plasmid for tagging *SWI4* with 3 Flag tags at its C terminus was constructed by gene synthesis (p623) followed by the insertion of an 880-bp PacI fragment containing *TRP1* (made by PCR using oligonucleotides 1223 and 1224 as primers and pRS414 [Stratagene] as a template) at a PacI site introduced into the 3′-UTR of *SWI4* to obtain p626. Yeast was transformed with a PmeI digest.

Expression plasmids for Swi4 and Swi6. A plasmid for expressing the first 202 residues of Swi4 followed by a 6-histidine tag and a single Flag tag (p618), based on pET28a(+) (Novagen), was constructed by replacing the entire XbaI-KpnI *SPT10* insert in p348 (38) with a 671-bp XbaI-KpnI *SWI4* fragment obtained by PCR: an initial PCR using yeast genomic DNA as a template and primers 1004 and 1005 was used to generate a template for use with primers 1229 and 1230. The N terminus of the Swi4-DBD is native. A plasmid for expressing full-length Swi4 with a native N terminus and C-terminal 6-histidine and Myc tags (p660) was constructed by replacing the SnaBI-KpnI fragment in p618 with a 3,186-bp SnaBI-KpnI fragment containing most of the *SWI4* ORF, made using yeast genomic DNA as a template and primers 1295 and 1296 to obtain p648 and then replacing the single Flag tag with a single Myc tag, inserted as a synthetic KpnI-XhoI double-stranded oligonucleotide (primers 1358 and 1359). An expression plasmid for full-length Swi6 with an N-terminal Flag tag and a C-terminal hemagglutinin (HA) tag (p659) was constructed by the insertion of the *SWI6* ORF obtained as a 2,490-bp NdeI-BamHI fragment using primers 1360 and 1361 into pET11a (Novagen).

Yeast strains. YPE250 (*MAT***a** *can1-100 his3-11 leu2-3,112 lys2*Δ *trp1-1 ura3-1 GAL*$^+$ *ADE2*$^+$ *SPT10-3HA*::*URA3*) was used for the reporter studies and was constructed by transforming a W303 wild-type strain with a SacI-HindIII digest of p355 (16) to tag *SPT10*. ChIP studies were performed with YPE334, contain-

TABLE 1. Oligonucleotides used in this work

Oligonucleotide	Sequence (5′→3′)
667	CATTAGCGCTGTTCCAAAATTTTCGCCTCACTGTGCGAAGCTATTGGAATGGAGTGTATT
668	AAATACACTCCATTCCAATAGCTTCGCACAGTGAGGCGAAAATTTTGGAACAGCGCTAAT
698	ATCGATTGCTTCATTCTTTT
711	CTGAATCTTTCGTTACCAAT
986	GGCGCGCTGCAGGGATCCCATTTTATATTTTATATGTATGAAATTTG
987	GGCGCGACTAGTGCTAGCCATTGTATGTGTGTATGGTTT
988	GGCGCGGGATCCGCTTCTTCTGAAGATGTCATCAC
989	GGCGCGCTGCAGTTACAAGAACAAGTGGTGTCTACC
990	GGCGCGGCTAGCATTCTGTCTAAAGGTGAAGAATTATTC
991	GGCGCGACTAGTTTAAGATCTTTTGTACAATTCATCCATACCATGG
992	GGCGCGACTAGTTAATGAAATCACTTCCTTTGGTTAT
993	GACGTTGCGGCCGCATTGTTCACACGAGCCAATG
994	GGCGCGCTGCAGTAAGATCGGTTCTGGTATTTTAAAGAAG
995	GGCGCGCTCGAGGACAGAAGCCGCGGGCT
996	GGCGCGAGATCTGCATCCAACTTGAACATTTCG
997	GGCGCGAGATCTCTATATTACTTGGGTATTGCC
1004	GGCGCGCATATGCCATTTGATGTTTTGATATCAAACC
1005	GGCGCGCTCGAGTTACTGGTTGATCGATGCATTTTTC
1010	P-GCTGACTCAAAATTCCTATCTCACTGTACAGGGCTATTGAGGTGGAGTGTATTTGGTGGCTC
1034	P-CCCTTTCTTCCGCGCGCAAATGATCCAGATGGATTTAAAATCAAGAGAATTG
1035	P-TGCAACGCGCTCCAAAGTGACTTAAGCCTTCCCTTTCGGGC
1036	CTACCAAGGCTTCTCAAGAATTAT
1037	GCAACAGAGAAAACAGGAAGACAC
1151	GGCGGCCCGCGGCTATGCCTCGGTAATGATTTTC
1152	GGCGGCCCGCGGCCGTTCAGAATGACACGTATAG
1192	CTGCTAAAGCCGAAAAGAAAC
1193	TTAGCCAATTCACCTGGTAAG
1223	CTCTTTAATTAAGTACAATCTTGATCCGGAGCT
1224	CTCTTTAATTAAGCAGGCAAGTGCACAAACAATA
1229	GGCGCGTCTAGAAATAATTTTGTTTAACTTTAAGAAGGAGATATACCATGCCATTTGATGTTTTGATATC
1230	GGCGCGGGTACCGTGATGATGATGATGATGTGAGCCCTGGTTGATCGATGCATTTTTC
1252	CATCGCGAAATTTGTCTCAAC
1253	GAAACATAACGGTTTTTGGCG
1254	CTCAATGTCGCCCGAAAG
1255	CTCTTGATTTTAAATCCATCGTTC
1280	TTCTCATTTCCCTTCTGTCCCTCTTGCGTAGTTCTAAAAGGTTGATTTATTCGAGAAATCCGGATCCCCGGGTTAATTAA
1281	AAAAAAATTTAAAAACTCTGATAATATAGTAAAAATTATTGGTACATTGTGAATTAAAATGAATTCGAGCTCGTTTAAAC
1282	GATCGAATTCATTTTAATTCACAATGTACCAATAAT
1283	ACATCTCAACTTGGATGATTCATTAC
1292	CAAATAAACCATACACACATACAATG
1293	P-ATCGTTAACGAAAGAGTTCAAG
1294	CTAGTATTTACGATCCACTGG
1295	P-GTATTCAGAAACCGATGTATACG
1296	GGCGCGGGTACCGTGATGATGATGATGATGTGAGCCTGC
1358	CGGTGAACAAAAGCTTATCTCCGAGGAAGACTTGAACTCTTAAC
1359	TCGAGTTAAGAGTTCAAGTCTTCCTCGGAGATAAGCTTTTGTTCACCGGTAC
1360	GGCGCGCATATGGGTACAGATTATAAAGATGACGATGACAAGGGTACCGCGTTGGAAGAAGTGGTAC
1361	GGCGCGGGATCCTCATGTACCAGCGTAATCTGGAAC
1409	CTATGGTTAGACGCTCAATGTCG
1410	CACTACTAAGGCCAATTCTCTTG
1413	GAACCTCAAAACTGCGTGTTC
1420	GTGCTCTTCGCTAGGTATCC
1425	TGGCGAAACCAATTTGTTCTCTCAA
1426	GGAGGATATATTACCTTTGATGTT
1501	GTAGCACGTCGCGTTTATGG
1502	GATGGCGCTCGTGATCCTG
1527	CCCGTATGGGACTCGTCAT
1528	AGTTGGCGAGGGGAACATT

ing both *SPT10-3HA* and *SWI4-3FLAG*, made by transforming YPE250 with a PmeI digest of p626 (*SWI4-3FLAG*::*TRP1*). The binding-site mutants were constructed by transforming YPE334 with an EcoRI-BamHI digest of p592 (WT), p656 (Spt10 half-site mutations), or p657 (Swi4 site mutations) to obtain YDC360, YDC361, or YDC362, respectively. In these strains, *HIS3* was integrated downstream of *HTA1*. The mutations were verified by the sequencing of PCR fragments containing the *HTA1-HTB1* promoter, obtained by PCR using genomic DNA from these strains. An *swi4*Δ strain (YPE352 [*MAT***a** *can1-100 ade2-1 his3-11 leu2-3,112 LYS2*$^+$ *trp1-1 ura3-1 GAL*$^+$ *swi4*Δ::*KanMX*]) was constructed by transforming a diploid W303 strain with an *swi4*Δ::*KanMX* fragment made by ligating two PCR fragments together (an *swi4*Δ::*KanMX* fragment was made by using primer pair 1280/1281 with pFA6a-KanMX6 [64] as a template, and a fragment containing 3′ *SWI4* sequences was made by using primer pair 1282/1283; both were digested with EcoRI, ligated together, and amplified by

using primer pair 1280/1283). The germination efficiency of *swi4*Δ spores was low; the resulting haploid cells were enlarged and tended to clump.

Reporter assay. Cultures (500 ml) were grown in synthetic medium without leucine to an A_{600} of ~0.2 and arrested using 10 μg/ml α-factor (a synthetic peptide corresponding to residues 104 to 120) for 2 h at 30°C. Cells were released from arrest by rapid filtration (0.45 μm) (Millipore HA), washed briefly with prewarmed medium, and resuspended in 500 ml prewarmed medium. Aliquots of cells were removed at various times, washed in cold water, and stored frozen. RNA was prepared by using the hot-phenol method, concentrations were determined spectrophotometrically, and RNA integrity was confirmed by ethidium staining of agarose gels. Northern blots of denaturing gels containing 2.5% formaldehyde were probed either with both 3′ *HTA1* and *ACT1* probes or with the *HTB1* coding region and GFP probes. Northern probes were PCR fragments radiolabeled by random priming: for 3′ *HTA1*, *ACT1*, and *CLN2* ORFs, primer pairs 1036/1037, 698/711, and 1527/1528, respectively, were used with yeast genomic DNA as a template; for the *HTB1* ORF, primer pair 1192/1193 was used with pCC67 as a template; and for GFP, primer pair 990/991 was used with pYM44 as a template. An aliquot of the same RNA sample was included on each blot for the normalization of GFP/*HTB1* signals. Phosphorimages were quantified by using ImageQuant software.

Purification of Spt10, the Swi4-DBD, and SBF. The purification of Spt10 using baculoviral expression was described previously (16). The Swi4-DBD was purified as follows. A total of 450 ml *Escherichia coli* BL21(DE3) cells transformed with p618 was grown to an A_{600} of ~0.6 in LB medium with 60 μg kanamycin/ml at 30°C and induced with 1 mM isopropyl-β-D-thiogalactopyranoside (IPTG) for 2 h. The cell pellet was resuspended in TI buffer (25 ml 50 mM Tris HCl [pH 8.0], 0.5 M NaCl, 0.1% Triton X-100, 5 mM 2-mercaptoethanol, 2 mM imidazole, and protease inhibitors without EDTA [catalog number 05056489001; Roche]) and lysed by 1 passage through a French press. The debris was removed by spinning at 10,000 rpm for 20 min in a Sorvall SA600 rotor. The supernatant was syringe filtered (0.45-μm Millex HA; Millipore), added to 2.5 ml Talon resin (Clontech) equilibrated in TI buffer, and mixed on a tube rotator for 20 min at 4°C. The resin was spun out, and the supernatant was removed. The resin was washed once with 10 ml TI buffer (10 min on rotator). An equal volume of TI buffer was added to the resin. The resuspension was transferred into a disposable gravity feed column. The column was washed with 5 ml TI buffer and eluted with a solution containing 150 mM imidazole, 20 mM Tris HCl (pH 8.0), 0.5 M NaCl, and 0.1% Triton X-100 containing protease inhibitors; 0.9-ml fractions were collected. The highly purified Swi4-DBD was obtained in an excellent yield (~10 mg). Its concentration was measured by using the Bradford assay (3a) with IgG as a standard. Swi4-6His-Myc and Flag-Swi6-HA were coexpressed in *E. coli* Rosetta 2(DE3)pLysS cells (EMD Biosciences) transformed with p659 (Kan^r) and p660 (Amp^r). Cells were grown to an A_{600} of ~1 in 1 liter LB medium containing 34 μg chloramphenicol/ml, 100 μg ampicillin/ml, and 40 μg kanamycin/ml at 30°C and induced for 4 h with 1 mM IPTG. The cells were lysed by sonication in 10 ml TI buffer. The extract was spun to remove debris and filtered, and Swi4 (with associated Swi6) was purified by using Talon resin as described above. To remove excess Swi4, Swi6 (with associated Swi4) was purified by affinity chromatography: the Talon peak fractions were pooled and mixed with 0.5 ml anti-Flag resin (catalog number A2220; Sigma) equilibrated in LS/LT buffer (0.15 M NaCl, 50 mM HEPES-K [pH 7.5], 0.2% Triton X-100, 1 mM Na-EDTA, and 10 μM pepstatin A with protease inhibitors) for 1 h at 4°C on a tube rotator. The resin was washed twice with LS/LT buffer containing 0.5 M NaCl–1% Triton X-100 and once with LS/LT buffer. SBF was eluted with 250 μl 1 mg 3-Flag peptide/ml (catalog number F4799; Sigma) in LS/LT buffer (the pH was adjusted to ~7 with 0.1 M HEPES-K [pH 7.5]). Elution was done for 60 min at 4°C on a tube rotator. The eluate was stored in aliquots at −80°C.

Gel shift experiments. The following probes were used: annealed oligonucleotides 667 and 668 (60 bp) for UAS1/UAS2, a 97-bp PCR fragment made using oligonucleotides 1254 and 1255 as primers and p526 as a template (mutated versions of this probe were obtained by using the same primers with plasmids containing the required mutations as templates) for UAS3/UAS4, and a 101-bp PCR fragment made using oligonucleotides 1252 and 1253 as primers and yeast genomic DNA as a template for the *CLN2* promoter. The PCR fragments were gel purified, and their concentrations were determined by measuring the A_{260}. Binding reactions were performed by using 5 nM radioactive probe in 15 μl of a solution containing 20 mM HEPES-K (pH 7.5), 70 mM NaCl, 5 mM $MgCl_2$, 10 μM zinc acetate, 0.1 mg/ml bovine serum albumin (BSA) (IgG-free) (catalog number A6918; Sigma), 0.05% Triton X-100, 10% glycerol, and 0.05 mg/ml poly(dI-dC) (catalog number P4929; Sigma) with protease inhibitors (as described above). After incubation at room temperature for 20 min, the reactions were analyzed in 6% (19:1) polyacrylamide gels containing 40 mM Tris-acetate (pH 8.3) and 5% glycerol. The binding of SBF was analyzed with 3.5% (50:1) polyacrylamide gels. Gels were electrophoresed at 150 V for ~2 h at room temperature using 40 mM Tris-acetate (pH 8.3) as a running buffer. Phosphorimages were quantified by using ImageQuant software.

ChIP experiments. ChIP experiments were performed as described previously (32), except for the following modifications. Cells (750 ml) were grown in synthetic complete (SC) medium to an optical density at 600 nm (OD_{600}) of ~0.5. Cultures were synchronized with α-factor (10 μg/ml) for 2 h at 30°C; 125 ml was removed for cross-linking. The remaining cells were washed to remove α-factor, resuspended in fresh medium (625 ml), and shaken at 30°C. Aliquots (125 ml) were removed at specific time points and fixed with 1% formaldehyde for 15 min at room temperature with shaking. Fixation was terminated by the addition of 100 ml 2.5 M glycine to the mixture and shaking for 5 min. Fixed cells were collected by filtration. Cross-linked chromatin was fragmented by using a Misonix Sonicator 3000 (96 pulses of 10 s separated by 10-s pauses for cooling), resulting in DNA fragments of ~250 bp on average (17). For immunoprecipitation reactions, 0.8 μg cross-linked chromatin (measured using a Hoechst assay) was mixed with protein G magnetic beads (catalog number 100.04; Dynal) carrying prebound M2-anti-Flag (catalog number F3165; Sigma) or anti-HA F7 (sc7392; Santa Cruz) monoclonal antibody. Elutions were performed by using specific peptides (3-Flag peptide) (catalog number F4799; Sigma) or HA peptide (catalog number 11666975001; Roche). Multiplex PCR was performed as described previously (32), using primer pair 1409/1410 to amplify UAS3/UAS4 as a 127-bp fragment, primer pair 1413/1420 for the *CLN2* promoter (82 bp), primer pair 1425/1426 for the *YLR454* ORF (105 bp), and primer pair 1501/1502 for the *HTA2-HTB2* promoter (163 bp).

RESULTS

Reporter assay for the effects of UAS mutations on *HTA1-HTB1* expression. A reporter plasmid was constructed in which all sequence elements important for *HTA1* and *HTB1* expression were retained (Fig. 1A). These are the four UAS elements, the NEG region located between UAS2 and UAS3, and the 3′-UTRs. In particular, the divergent promoter organization was preserved. In effect, the open reading frames encoding H2A (*HTA1*) and H2B (*HTB1*) were replaced with those encoding the fluorescent proteins RedStar-2 (RDS2) (30) and GFP, respectively. The modified *HTA1-HTB1* locus was inserted into a single-copy *CEN ARS LEU2* plasmid.

Our original plan was to measure the output of the reporters by measuring RDS2 and GFP fluorescence. However, this did not work well, perhaps because of slow protein maturation or turnover (3). Instead, reporter expression was measured by hybridizing Northern blots with probes corresponding to the 3′-UTRs of *HTA1* and *HTB1*. This had the advantage that the probe detects both the reporter and the endogenous transcripts, facilitating quantitative comparisons of reporter expression relative to the endogenous *HTA1-HTB1* locus. Although this approach worked well for RDS2/*HTA1*, it was not quantitatively reliable for GFP/*HTB1*, probably because the 3′-*HTB1* probe is extremely AT rich. For *HTB1* and GFP, separate coding-region probes were used; the relative amounts were determined by probing all blots with the same probe preparations or by including a reference sample.

Yeast cells transformed with the reporter plasmid were synchronized using α-factor, which arrests cells in the G_1 phase of the cell cycle. The cell cycle dependence of RDS2 and *HTA1* expression in cells carrying a reporter plasmid containing a wild-type *HTA1-HTB1* promoter is shown in Fig. 1B and quantified in Fig. 1C (left). In both cases, two peaks of expression were observed: the first peak occurred ~30 min after α-factor release, and the second peak occurred after ~90 to 100 min. The expression profile for RDS2 was qualitatively very similar to that of endogenous *HTA1*. The amount of RDS2 mRNA

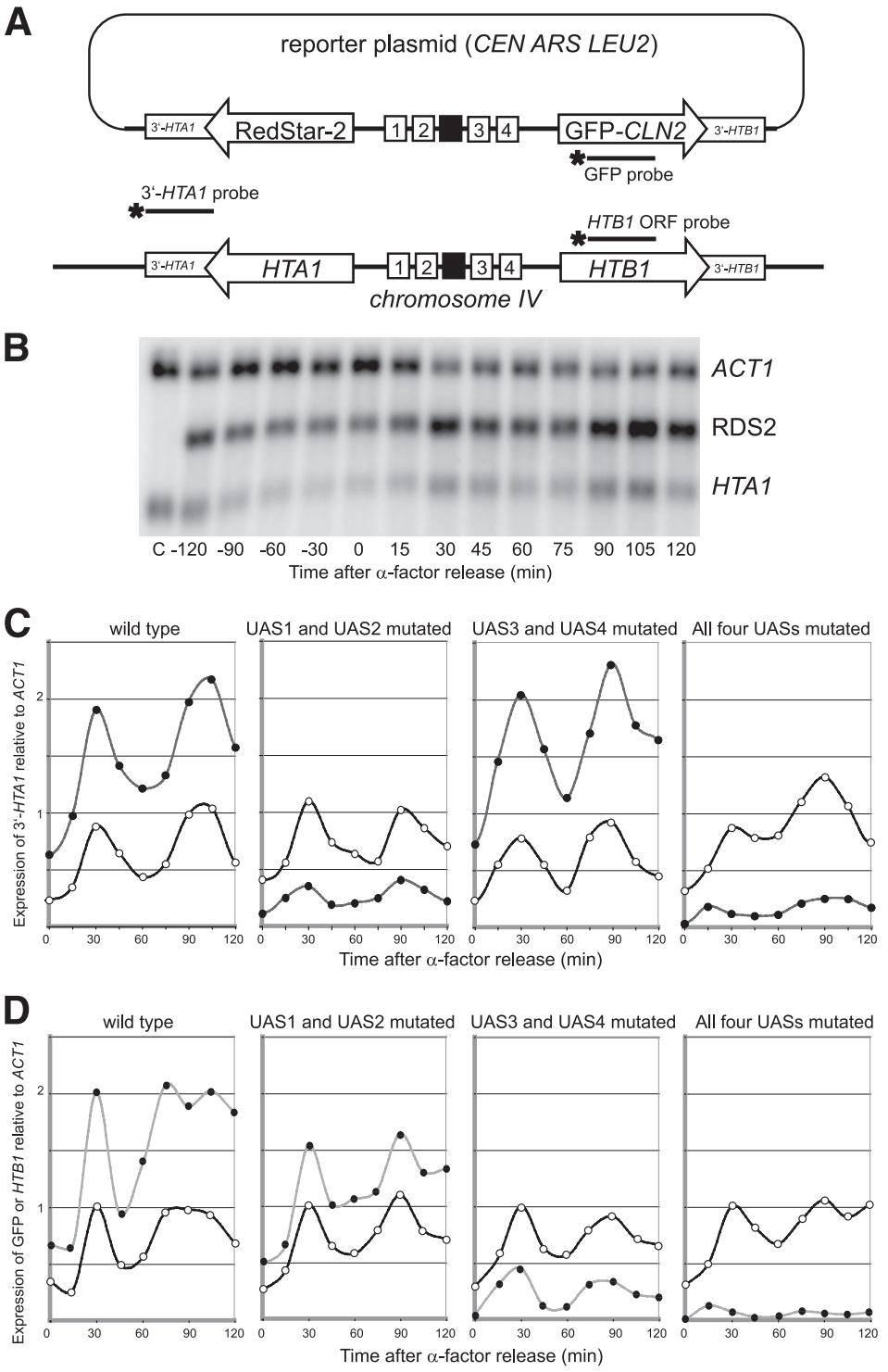

FIG. 1. The UAS elements direct the cell cycle-dependent activation of *HTA1-HTB1*. (A) Reporter plasmid for assaying mutations in the *HTA1-HTB1* promoter. The coding regions of *HTA1* and *HTB1* were replaced with RDS2 and GFP fused to PEST sequences from *CLN2*, respectively. Numbered boxes, UAS elements; black box, NEG region. RDS2 and *HTA1* mRNAs were detected by using a single probe (3′-UTR of *HTA1*). Separate GFP and *HTB1* probes were used for *HTB1*. (B) Cells were synchronized by using α-factor. Shown is a typical Northern blot probed for 3′ *HTA1* and *ACT1*. C, RNA from a strain lacking a reporter plasmid. (C) Expression of RDS2 (filled circles) and *HTA1* (open circles) in cells carrying the wild-type reporter or reporters with UAS1 and UAS2 mutated, UAS3 and UAS4 mutated, or all four UAS elements mutated. Relative levels of RDS2 and *HTA1* may be compared because the same probe was used to detect both transcripts. (D) Expression of GFP (filled circles) and *HTB1* (open circles). All four blots were hybridized at the same time with the same GFP/*HTB1* probe mix to allow a direct comparison of GFP signals in each strain.

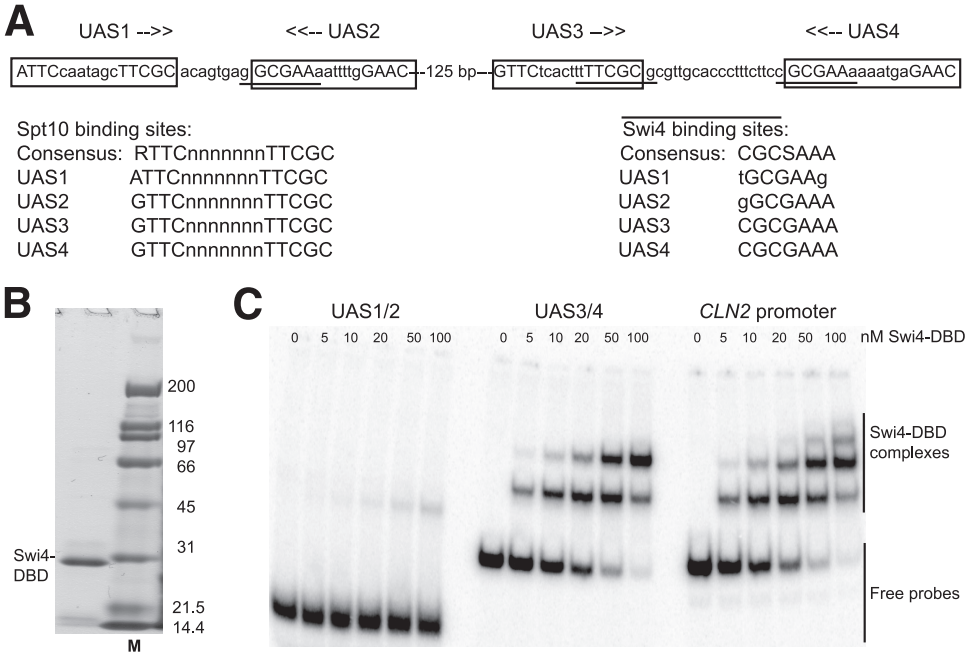

FIG. 2. The DNA binding domain of Swi4 binds specifically and with high affinity to UAS3 and UAS4 but not to UAS1 and UAS2. (A) Spt10 and Swi4 binding sites in the *HTA1-HTB1* promoter. Uppercase type indicates bases important for Spt10 binding. Putative Swi4 binding sites are underlined. Spt10 and Swi4 sites are listed (lowercase type indicates deviations from the consensus). (B) Purified Swi4 DNA binding domain analyzed in a protein gel stained with Coomassie blue. M, marker. (C) Gel shift assay for binding of the Swi4-DBD using a 67-bp probe containing UAS1 and UAS2, a 97-bp probe containing UAS3 and UAS4, and a 101-bp probe with part of the *CLN2* promoter (positive control). The Swi4-DBD gives two complexes with UAS3/UAS4, corresponding to the occupation of one or both binding sites. The *CLN2* probe contains at least three Swi4 sites.

was approximately double that of *HTA1*, for reasons which are unclear. GFP and *HTB1* were expressed in a qualitatively similar manner: both gave peaks at ~30 min and ~90 min after α-factor release (Fig. 1D). Thus, the reporter genes behaved very similarly to the endogenous genes.

UAS1 and UAS2 drive *HTA1*, and UAS3 and UAS4 drive *HTB1*, with some cross talk. We have shown previously that Spt10 is a dimer and that it requires two UAS elements to bind with high affinity (16, 39). Therefore, the contributions of the four UAS elements to *HTA1* and *HTB1* expression were determined by mutating pairs of UAS elements: either UAS1 and UAS2 or UAS3 and UAS4. All but one of the bases important for Spt10 binding were mutated in each UAS. The mutation of UAS1 and UAS2 (UAS3 and UAS4 intact) reduced RDS2 expression to only ~15% of that of the wild-type reporter (Fig. 1C). In contrast, the level of GFP expression was only mildly reduced when UAS1 and UAS2 were mutated (to ~75% of that of the wild type) (Fig. 1D). Thus, UAS1 and UAS2 are of major importance for the expression of *HTA1*/RDS2 but have only a minor effect on *HTB1*/GFP. The mutation of UAS3 and UAS4 (UAS1 and UAS2 intact) had essentially no effect on RDS2 expression but reduced GFP expression to just ~25% of that of the wild type (Fig. 1C and D). Thus, UAS3 and UAS4 are of major importance for the expression of *HTB1*/GFP but have no effect on *HTA1*/RDS2, the opposite effect of the UAS1 and UAS2 mutations. Mutations in all four UAS elements resulted in just a small amount of residual expression of both reporter genes, although this residual expression was clearly cell cycle dependent and perhaps slightly early, peaking at 15 min. The residual expression was at levels significantly below those observed for mutations in two of the four UAS elements, revealing that UAS1 and UAS2 have a small but significant effect on *HTB1*/GFP and confirming that UAS3 and UAS4 have a relatively minor effect on *HTA1*/RDS2. In conclusion, UAS1 and UAS2 primarily drive *HTA1* and UAS3 and UAS4 primarily drive *HTB1*, but each pair of UAS elements has a small but significant stimulatory effect on the more distant gene.

Swi4 binding sites in UAS3 and UAS4 overlap the Spt10 binding sites. Initially, we attributed the effects of mutations in the UAS elements to Spt10. However, there are predicted binding sites for Swi4 (SBF) that are almost entirely contained within the UAS elements (Fig. 2A). Two closely related Swi4 consensus sites have been suggested: CACGAAAA (60) and CGC(C/G)AAA (26). There are no exact matches to the former consensus in the *HTA1-HTB1* promoter, but UAS3 and UAS4 both contain the sequence CGCGAAA, an exact match to the latter consensus. In addition, UAS1 and UAS2 contain related sequences (TGCGAAG and GGCGAAA, respectively).

To determine whether the predicted Swi4 binding sites are actual sites, the Swi4-DBD, corresponding to the N-terminal 202 residues (63), was prepared for gel shift analysis (Fig. 2B). A 101-bp DNA fragment corresponding to part of the *CLN2* promoter containing three Swi4 binding sites (47) was used as a positive control (Fig. 2C). As expected, the Swi4-DBD bound with high affinity to the *CLN2* promoter: three complexes were observed, corresponding to the binding of one, two, and three

Swi4-DBD molecules to the same DNA molecule. Analysis of the binding data revealed that there are two high-affinity sites in the *CLN2* promoter with a K_d (dissociation constant) of 15 ± 6 nM ($n = 2$) and a Hill coefficient close to 1, indicating that these sites are essentially independent. The third site appeared to have a significantly lower affinity. A much weaker binding (K_d of ~800 nM) was reported for N-terminal fragments of Swi4 to an oligonucleotide containing one of the *CLN2* promoter sites (63); it is unclear why our Swi4-DBD binds with a much higher affinity.

The Swi4-DBD bound with similar affinity to a 97-bp fragment containing both UAS3 and UAS4, yielding two complexes corresponding to binding to one or both UAS elements ($K_d = 25 \pm 6$ nM; $n = 4$). Analysis of the binding data for UAS3 and UAS4 yielded a Hill coefficient close to 1, indicating that the Swi4-DBD binds independently to UAS3 and UAS4; i.e., it binds noncooperatively. This was consistent with a K_d of ~18 nM measured for UAS3 in a DNA fragment carrying mutations in UAS4. In contrast, the Swi4-DBD bound extremely weakly to a 67-bp fragment containing UAS1 and UAS2 (Fig. 2C), indicating that these are very-low-affinity sites (K_d of >500 nM), presumably reflecting the mismatches to the consensus sequence. In conclusion, the fragment containing UAS3 and UAS4 contains two high-affinity binding sites for the Swi4-DBD, whereas the binding of the Swi4-DBD to the fragment containing UAS1 and UAS2 is so weak that it is unlikely to be biologically significant.

Spt10 and SBF compete for binding to UAS3 and UAS4. There is extensive overlap between the binding sites for Spt10 and Swi4 in UAS3 and UAS4: both Swi4 sites (TTTCGCG on the opposite strand) overlap the downstream half of the bipartite site recognized by Spt10 (GTTC-N_7-TTCGC) (Fig. 2A). This overlap is so extensive that it seemed likely that the binding of Spt10 and binding of Swi4 would be mutually exclusive; i.e., they would compete for binding to UAS3 and UAS4. However, in a competition gel shift experiment in which increasing amounts of Spt10 were mixed with sufficient Swi4-DBD to bind almost all of the probe, additional complexes were observed (Fig. 3A). This indicated that, surprisingly, both Spt10 and the Swi4-DBD could bind to the same DNA molecule, presumably by binding on opposite sides of the DNA helix. However, the Swi4-DBD is much smaller than the SBF complex (Swi4 has 1,093 residues, and Swi6 has 803). Therefore, SBF might inhibit the binding of Spt10 through much increased steric hindrance. To test this hypothesis, recombinant SBF was prepared by the coexpression of Swi4 (with C-terminal 6-histidine and Myc tags) and Swi6 (with an N-terminal Flag tag and a C-terminal HA tag) in *E. coli*. The Swi4-Swi6 complex was affinity purified first by immobilized metal affinity chromatography to obtain Swi4 and then by using anti-Flag resin to obtain Swi4 bound to Swi6. Although both of these large proteins were susceptible to degradation, reasonably pure recombinant SBF was obtained (Fig. 3B).

The binding of SBF to the probe containing both UAS3 and UAS4 was analyzed in gel shift experiments (Fig. 3C). It was necessary to use a probe with two UAS elements, because Spt10 requires two such elements for high-affinity binding (16). To resolve the complexes, very-low-percentage polyacrylamide gels were used (the Swi4-Swi6 heterodimer has a molecular weight of ~215,000); these had the unfortunate property of causing the DNA to smear somewhat in the presence of SBF. SBF formed four complexes on the UAS3/UAS4 probe. The two lower complexes were attributed to Swi4-Swi6 degradation products, the major band was attributed to the binding of SBF to either UAS3 or UAS4, and the weak upper band was attributed to the binding of a second SBF at the second UAS. This interpretation is based on the fact that the upper complex did not appear when a probe with mutations in UAS4 was used (not shown). The binding of SBF appeared to be negatively cooperative, unlike that of the Swi4-DBD (Fig. 2C), presumably due to a steric hindrance of the binding of a second SBF by the first. The analysis of SBF binding to UAS3/UAS4 gave a K_d of ~120 nM. This is significantly higher than that of the Swi4-DBD ($K_d = 25$ nM), but the smearing of DNA in the gel complicated the measurement of the K_d, and some of the SBF might be inactive.

To determine whether both SBF and Spt10 can bind to the UAS elements at the same time, or whether they compete for binding, gel shift experiments were performed in which sufficient SBF to bind almost all of the probe was mixed with increasing amounts of Spt10 prior to the addition of the DNA (Fig. 3C). As Spt10 was titrated in, complexes corresponding to the binding of Spt10 alone appeared in increasing amounts, and concomitantly, the complexes corresponding to the various SBF complexes decreased, indicating that SBF and Spt10 compete for binding to UAS3 and UAS4. The same result was obtained when SBF was mixed with DNA for 10 min before the addition of Spt10 and when Spt10 was mixed with DNA before the addition of SBF (not shown), indicating that the binding of both factors is reversible. In conclusion, the binding of SBF and binding of Spt10 to UAS3 and UAS4 are mutually exclusive.

Binding-site mutations in UAS3 and UAS4, which discriminate between Spt10 and Swi4. The fact that UAS3 and UAS4 contain high-affinity sites for Swi4 presents a problem for the interpretation of the reporter experiments (Fig. 1), because the UAS mutations described above would prevent the binding of Swi4 as well as that of Spt10. This is in fact the case (Fig. 4). Spt10 bound with moderately high affinity to UAS3 and UAS4 ($K_d = 81 \pm 8$ nM; $n = 2$), which is somewhat weaker than that for binding to UAS1 and UAS2 ($K_d = 45$ nM) (16). The lower affinity of Spt10 for UAS3/UAS4 than that for UAS1/UAS2 might be due to the difference in distance between the UAS elements (6 bp between UAS1 and UAS2 and 17 bp between UAS3 and UAS4). As expected (16), Spt10 did not bind at all to the mutated UAS elements used in the reporter assay (Fig. 4B). The level of binding of the Swi4-DBD to the fully mutated UAS elements was strongly reduced (K_d of ~200 nM, corresponding to a ~10-fold reduction in affinity) but, surprisingly, was not completely eliminated (Fig. 4C). This is probably due to the accidental creation of two weak binding sites with one mismatch to the consensus, both of which include some flanking bases and some bases within mutated UAS4 (CGCGCAA and CGCGGAA).

New UAS mutations to discriminate between the binding of Swi4 and that of Spt10 were designed. Spt10 binding was eliminated without affecting Swi4 binding by mutating all four bases in each upstream half-site (GTTC), which does not overlap with the Swi4 site (Fig. 4A and B). The elimination of Swi4 binding without affecting Spt10 binding was more challenging, because the downstream Spt10 half-site includes all but the

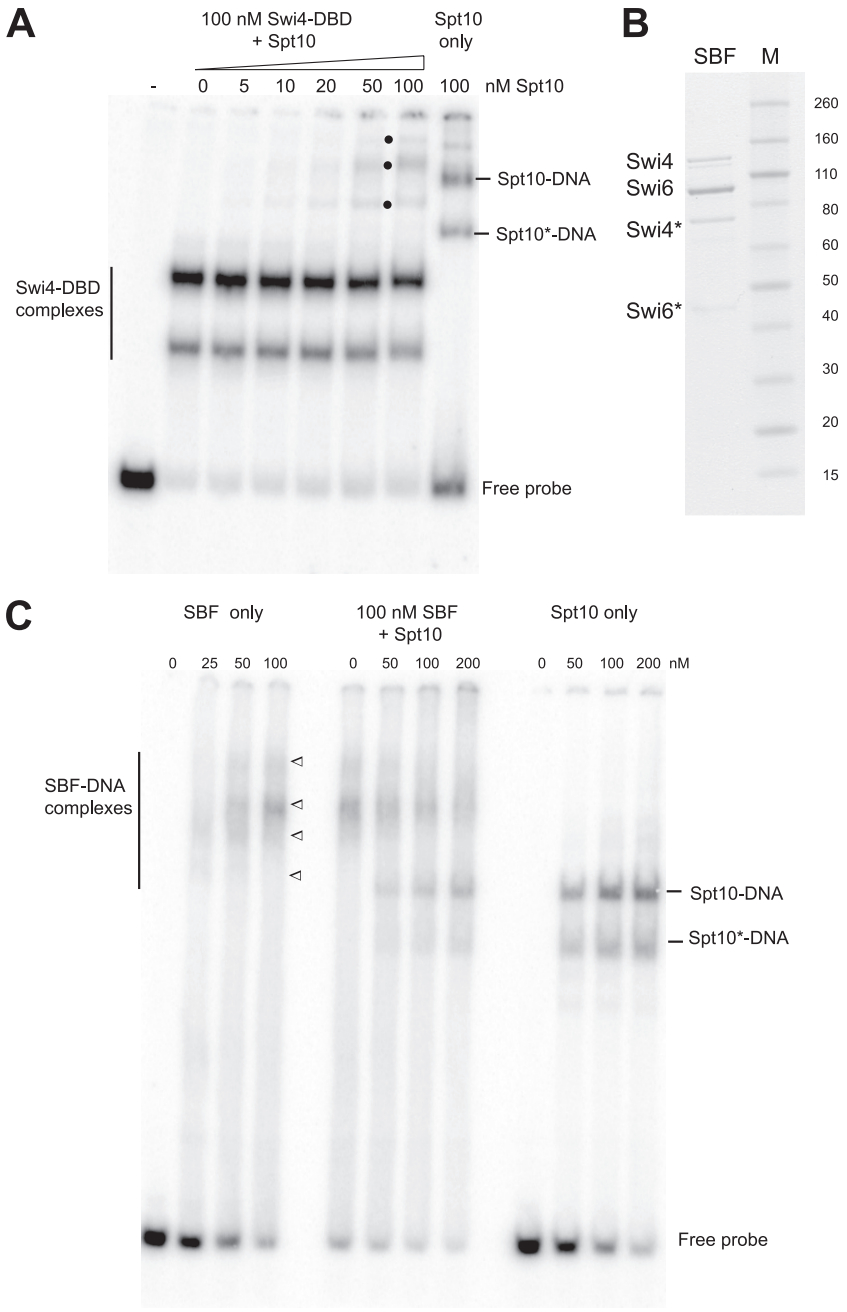

FIG. 3. SBF and Spt10 compete for binding to UAS3 and UAS4. (A) Simultaneous binding of the recombinant Swi4-DBD and Spt10 to a 97-bp probe containing UAS3 and UAS4. The Swi4-DBD was fixed at 100 nM; Spt10 was added in increasing amounts. Bullets indicates complexes formed only in the presence of both proteins. Spt10* indicates degraded Spt10. (B) Recombinant SBF analyzed in a protein gel stained with Coomassie blue. Swi4* and Swi6* indicate degradation products. (C) Competition between SBF and Spt10 for binding to the UAS3/UAS4 probe. Increasing amounts of Spt10 were mixed with a fixed amount of SBF, and DNA was then added. For SBF-DNA complexes, the upper band is the probe with two SBFs bound, the upper middle complex is the probe with one SBF bound, and the lower middle and lower complexes are the degraded forms of SBF.

outermost bases of the Swi4 site: T(TTCGC)G. The mutation of both outermost bases to G(TTCGC)T eliminated the binding of the Swi4-DBD but also had a small but significant effect on Spt10 binding (not shown). However, a mutation of the downstream G to C had a major effect on the binding of the Swi4-DBD (K_d of >500 nM), a >40-fold reduction in affinity, without affecting Spt10 binding (Fig. 4B and C). The mutation of this G to A had less effect on affinity (K_d of ~100 nM). In conclusion, the mutation of the upstream half-site recognized by Spt10 prevents Spt10 binding without affecting that of Swi4, and the mutation of the Swi4 site from CGCGAAA to GGC GAAA severely reduces the binding of Swi4 without affecting that of Spt10. Thus, these mutations can be used to discriminate between the functions of Spt10 and Swi4 *in vivo*.

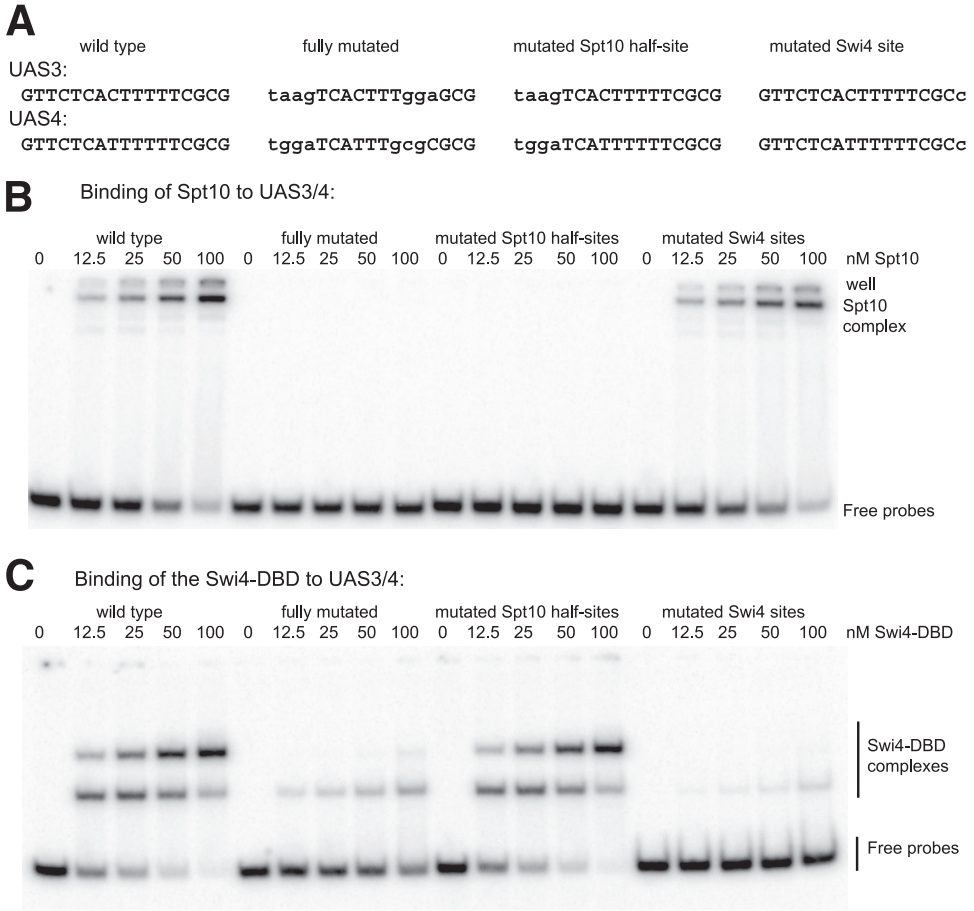

FIG. 4. Binding-site mutations in UAS3 and UAS4 which discriminate between Spt10 and Swi4 binding *in vitro*. (A) Mutations (lowercase type) in UAS3 and UAS4 tested for binding by Spt10 or Swi4. Fully mutated indicates mutations tested in the reporter assay (Fig. 1). (B) The Spt10 half-site mutations in UAS3 and UAS4 abolish Spt10 binding *in vitro*, and the Swi4 site mutations do not affect Spt10 binding. Gel shift assays used a series of 97-bp probes. (C) Mutations in the Swi4 sites strongly reduced the binding of the Swi4-DBD, and mutations in the Spt10 half-sites do not affect Swi4-DBD binding.

Effects of mutating the Spt10 or Swi4 binding sites in the chromosomal *HTA1-HTB1* locus *in vivo*. The Spt10 upstream half-site mutations were introduced into all four UAS elements in the native *HTA1-HTB1* locus. This strain exhibited a marked growth phenotype: its doubling time in synthetic complete (SC) medium was 2.8 h, whereas the doubling time of the wild type was only 1.7 h (Fig. 5A). This result confirms that Spt10 plays a major role in the regulation of *HTA1-HTB1* and shows that Swi4 cannot compensate for the loss of Spt10 function. Another strain, in which point mutations were introduced into UAS3 and UAS4, changing both Swi4 sites from CGCGAAA to GGCGAAA, was constructed. This strain did not have a significant growth defect (doubling time = 1.7 h) (Fig. 5A), indicating that the contribution of SBF to *HTA1-HTB1* regulation is more subtle than that of Spt10.

The effectiveness of these mutations in preventing the binding of Spt10 or Swi4 *in vivo* was determined by ChIP using a yeast strain expressing Spt10 with three C-terminal HA tags and Swi4 with three C-terminal Flag tags (Fig. 5B and C). The presence of Spt10-3HA at the *HTA1-HTB1* locus in wild-type cells was confirmed by a strong ChIP signal. Spt10-3HA was not detectable in the middle of the *YLR454* gene, which served as a negative control. The Spt10 half-site mutations eliminated the binding of Spt10-3HA at the *HTA1-HTB1* promoter, as expected. Surprisingly, the binding of Spt10 at the *HTA2-HTB2* promoter, used as a positive control, was also strongly reduced in this mutant (~4-fold). This might indicate that the nuclear Spt10 concentration is lower in the half-site mutant cells, presumably as an indirect result of the poor growth of this strain. Clearly, the loss of the Spt10-dependent activation of *HTA1-HTB1* is not compensated for by increased Spt10 binding at *HTA2-HTB2*. The mutation of the Swi4 sites in UAS3 and UAS4 did not have a significant effect on the binding of Spt10 at *HTA1-HTB1* (Fig. 5C). This finding suggests that Swi4 does not compete strongly with Spt10 in arrested cells, because mutations preventing Swi4 binding might be expected to increase Spt10 binding, if that were the case. However, competition between Spt10 and Swi4 at UAS3/UAS4 might be masked by Spt10 binding at UAS1/UAS2, since the distance between UAS2 and UAS3 is only 125 bp, and the average size of the chromatin fragments used in these ChIP experiments was ~250 bp.

As expected, Swi4 was also clearly detectable at the *HTA1-HTB1* promoter. However, the Swi4 signal at the *CLN2* pro-

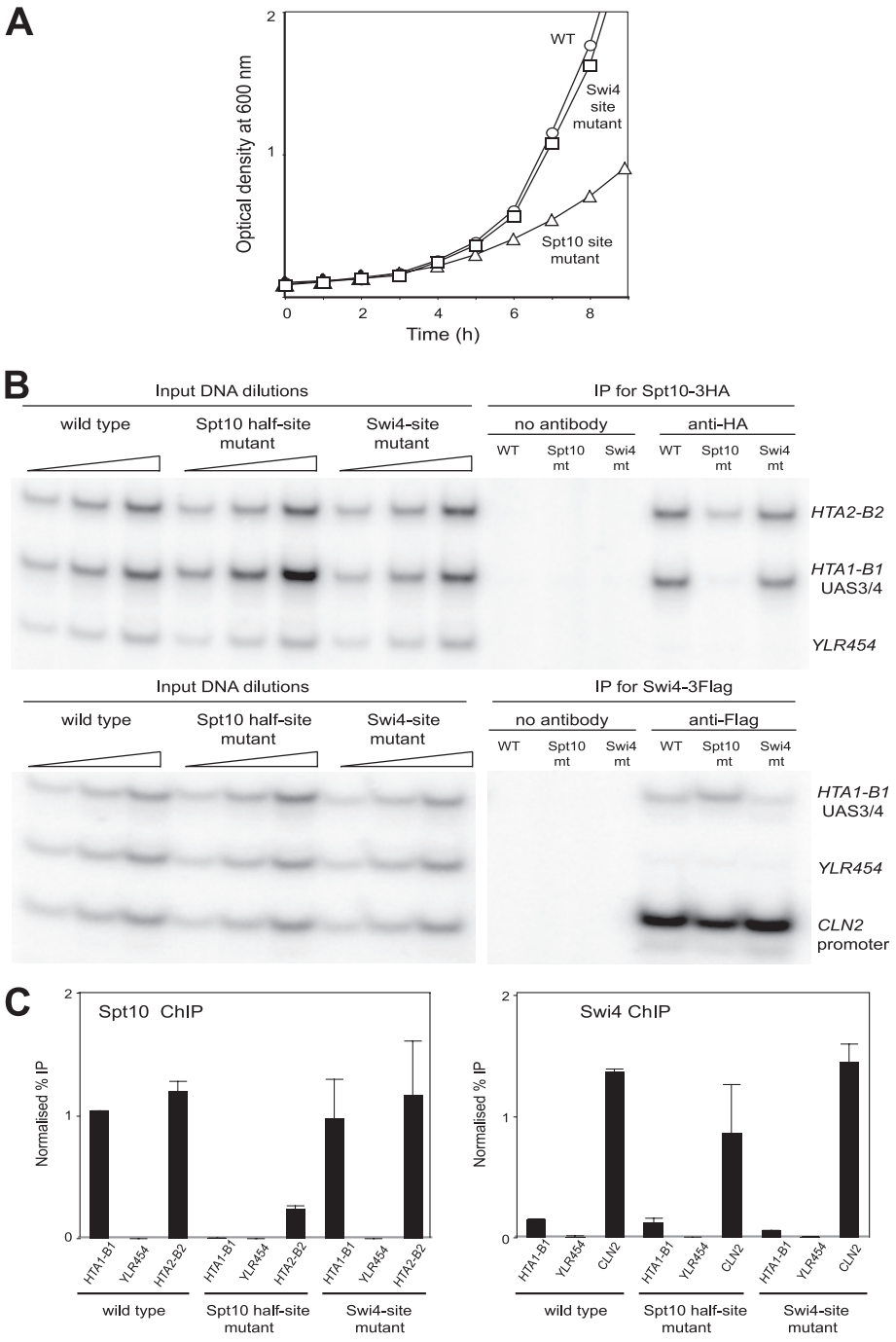

FIG. 5. Effects of introducing Spt10 and Swi4 binding-site mutations at the chromosomal *HTA1-HTB1* locus *in vivo*. (A) Growth in SC medium of strains carrying Spt10 half-site or Swi4 site mutations at the chromosomal *HTA1-HTB1* locus. (B) Binding of Spt10 and Swi4 in cells arrested with α-factor. Shown are data for ChIP using a strain expressing Spt10-3HA and Swi4-3Flag. Multiplex PCR analysis was done using primers for UAS3/UAS4 in *HTA1-HTB1* and for the coding region of *YLR454* (negative control). Positive controls were the *HTA2-HTB2* promoter for Spt10 and the *CLN2* promoter for Swi4. Phosphorimages are shown (in the case of Swi4, some lanes between the inputs and the test samples have been removed). (C) Quantitation of ChIP data. Error bars indicate standard deviations for two independent experiments.

moter, used as a positive control, was ~10-fold higher than that at *HTA1-HTB1*. This large quantitative difference might indicate that the occupancy of the Swi4 sites in the *HTA1-HTB1* promoter is much lower than that of the Swi4 sites in the *CLN2* promoter, even though these sites have very similar affinities for Swi4 (Fig. 2C). However, the fact that the *CLN2* promoter contains five predicted high-affinity Swi4 sites (located between positions −605 and −473 relative to the *CLN2* start codon), whereas *HTA1-HTB1* has only two such sites, must also be taken into account. The point mutations in UAS3 and UAS4 reduced the Swi4 signal by ~2-fold and had no significant effect on Swi4 binding at the *CLN2* promoter (Fig.

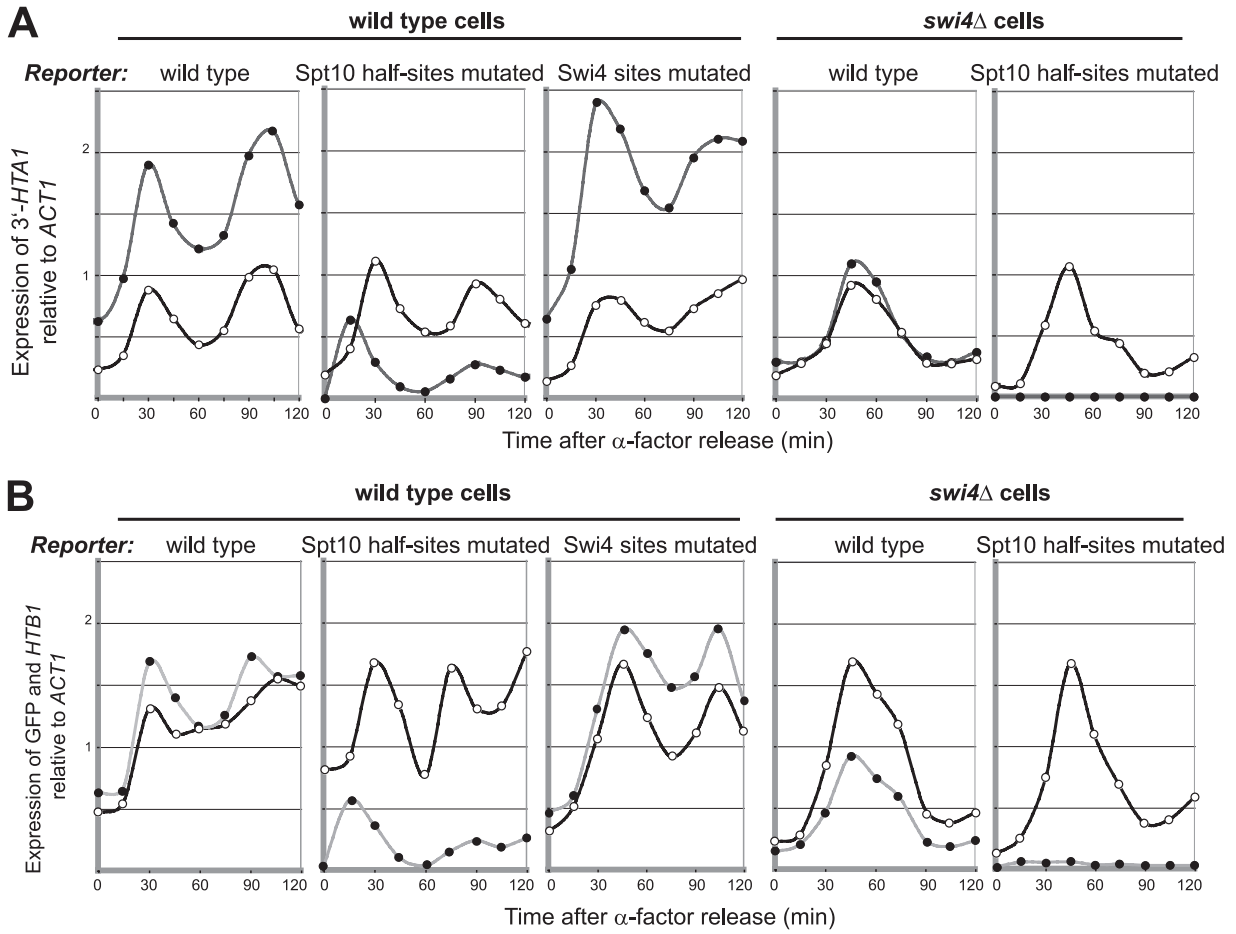

FIG. 6. Mutations preventing the binding of Spt10 result in a small, early, Swi4-dependent peak of *HTA1* and *HTB1* expression. (A) Effects of mutations in the Spt10 half-sites in all four UAS elements, or the Swi4 sites in UAS3/UAS4, on the cell cycle-dependent expression of RDS2 (filled circles) and *HTA1* (open circles) in synchronized WT or *swi4*Δ cells. (B) Effects of the same mutations on GFP (filled circles) and *HTB1* (open circles) expression. GFP levels in each of the strains may be compared directly, because the signals were normalized to a common RNA sample used as a standard in all of the blots. The same RNA samples were used for panels A and B.

5C). The Swi4 site mutations were less effective than expected, given the large decrease in affinity observed *in vitro* (Fig. 4C), but it should be noted that the level of the signal observed for the Swi4 site mutant was close to background levels (Fig. 5B). The mutation of the Spt10 sites did not result in an increased binding of Swi4 at UAS3/UAS4, as would be expected for a simple competition. However, the binding of Swi4 at the *CLN2* promoter was significantly reduced relative to that of wild type cells (Fig. 5C), as observed for Spt10 binding at *HTA2-HTB2*, suggesting that cell cycle regulation is generally compromised in these slow-growing cells.

In conclusion, UAS mutations that discriminate between Spt10 and Swi4 binding at the *HTA1-HTB1* promoter have been described.

Spt10 is responsible for the major cell cycle-dependent peak in *HTA1-HTB1* expression, whereas Swi4 drives a small, early peak of expression. The effects of the Spt10 upstream half-site and Swi4 site mutations on reporter expression were determined (Fig. 6). In the case of *HTA1*/RDS2, the mutation of the Spt10 half-sites resulted in a large reduction in expression and a shift in the peak of expression: a small, early, peak was observed 15 min after α-factor release, instead of a major peak at ~30 min (Fig. 6A). The same was observed for *HTB1*/GFP (Fig. 6B). The difference between the wild type and the Spt10 half-site mutant represents the contribution of Spt10 to the regulation of *HTA1* and *HTB1*. Thus, Spt10 is required for most of the cell cycle-dependent expression of *HTA1* and *HTB1*. The implication is that the small, early peak is due to Swi4. To determine whether this peak is dependent on Swi4, the reporter carrying the Spt10 half-site mutations was assayed in an *swi4*Δ strain (Fig. 6). The expression of the endogenous *HTA1* and *HTB1* genes was delayed relative to that of wild-type cells, peaking 15 min later, at ~45 min after α-factor release. This is consistent with the slow-growth phenotype exhibited by the *swi4*Δ strain, which represents an extension of the cell cycle. In contrast, the Spt10 site mutations abolished the expression of RDS2, and GFP expression was reduced to very low levels, confirming that Swi4 is indeed required for the small, early peak of expression.

In wild-type cells, the level of expression of RDS2 and GFP from a reporter plasmid carrying the Swi4 site mutations in UAS3 and UAS4 was somewhat higher than that for the wild-

type reporter (Fig. 6), but this difference is probably within experimental error. There was no obvious effect on the shape of the peak at early times, but the expected loss of the small peak in expression due to Swi4 would be difficult to measure in the presence of the major peak due to Spt10. However, the Swi4 site mutations did have an effect on the timing of the GFP peak, which shifted from ~30 min to ~45 min, and there might also be a small shift in the RDS2 peak to later times, although this might be within experimental error. Remarkably, this shift was also observed for endogenous *HTB1* expression, which has a wild-type promoter, suggesting an effect of the reporter mutations in *trans*. There was also an effect on the timing of endogenous *HTB1* expression in the Spt10 half-site mutant reporter, such that the second cycle was earlier than that for the wild-type reporter. These observations are being investigated further. In conclusion, Swi4 appears to initiate the cell cycle-dependent expression of *HTA1* and *HTB1*, driving a small, early peak in expression, which is followed soon after by an overlapping and much larger peak of expression driven by Spt10.

Cell cycle-dependent binding of Spt10 and Swi4 at the *HTA1-HTB1* promoter. To determine whether the peaks of *HTA1* and *HTB1* expression correlate with the binding of Spt10 and Swi4, their presence at the *HTA1-HTB1* promoter was measured by ChIP as a function of time (Fig. 7). Cells containing both Spt10-3HA and Swi4-3Flag were synchronized with α-factor in the same way as described above for the reporter assays. Spt10 was bound at UAS3/UAS4 at relatively high levels in cells arrested with α-factor, eventually declining to just ~20% of the initial level ~60 min after α-factor release (Fig. 7A and B), coinciding with the low point of *HTA1-HTB1* expression. Thus, the amount of Spt10 bound at the *HTA1-HTB1* promoter was highest within 15 min of α-factor release, coinciding with increasing expression levels of the genes, but there was no obvious peak in Spt10 binding. This was also the case for Spt10 binding at UAS1/UAS2 (not shown). Thus, the correlation between Spt10 binding and *HTA1*/*HTB1* expression is not exact, since Spt10 was bound at maximal levels in arrested cells, when the level of expression was low (Fig. 7C).

The time course of the binding of Swi4 at UAS3/UAS4 and the *CLN2* promoter indicated that it was bound at high levels in cells arrested with α-factor, like Spt10 (Fig. 7A and B). However, unlike Spt10, the Swi4 signal increased after α-factor release, showing a clear peak in binding at *HTA1-HTB1* between 7.5 and 15 min (this peak appeared slightly later at the *CLN2* promoter, at 15 min) and then declining steeply to very low levels after 60 min. The binding profile for Swi4 at *HTA1-HTB1* is consistent with expression due to Swi4 in that it peaks concurrently with, or just before, the small, early expression peak at 15 min (Fig. 7C). However, as for Spt10, the level of binding of Swi4 at *HTA1-HTB1* and *CLN2* was rather high in arrested cells, even though they expressed *HTA1* and *HTB1* at low levels. This implies that both Spt10 and Swi4 are bound in a poised state in G_1 phase, awaiting a signal to activate expression.

In additional ChIP experiments, the time course was extended to include a second cell cycle, but the expected second peaks for both Spt10 and Swi4 were much reduced and broadened relative to those of the first cycle (not shown). Concurrent RNA analysis indicated that *HTA1* and *HTB1* showed the expected periodic expression (Fig. 7D). However, *CLN2* mRNA clearly peaked before the histone mRNAs in the first cycle but was coincident with them in the second cycle. This indicates a significant loss of synchrony in the second cycle and suggests an explanation for the broadened ChIP signals. This conclusion is supported by a fluorescence-activated cell sorter (FACS) analysis performed in parallel (not shown).

DISCUSSION

In summary, we have shown that the UAS elements are required for virtually all expression of *HTA1* and *HTB1*. UAS1 and UAS2 primarily drive *HTA1*, whereas UAS3 and UAS4 primarily drive *HTB1*. Thus, each UAS pair has its greatest effect on the closest gene. There is some cross talk: UAS1 and UAS2 have a minor activating effect on *HTB1*, and UAS3 and UAS4 have a similar effect on *HTA1*. Most of the transcription is activated by Spt10, but a small peak in the expression of both genes, occurring earlier than the Spt10-dependent peak, is due to SBF, working through sites in UAS3 and UAS4. A role for SBF in *HTA1-HTB1* regulation is supported by the demonstration that the predicted Swi4 sites in UAS3 and UAS4 are indeed high-affinity sites for Swi4 and SBF *in vitro*, that these sites are occupied *in vivo*, and that the small early peak is dependent on Swi4. However, the role of Spt10 in *HTA1-HTB1* regulation is much more important, as shown by the fact that UAS mutations which prevent the binding of Spt10 eliminate most of the reporter expression, sparing only the small, early, Swi4-dependent peak, and result in a quite severe growth phenotype when introduced into the chromosomal *HTA1-HTB1* locus (even though *HTA2-HTB2*, the other locus encoding H2A and H2B, remains intact). The severity of this growth phenotype is similar to that observed previously for an *hta1-htb1*Δ strain (45), although it is not as severe as that of an *spt10*Δ strain, as expected, since the latter affects the expression of all four major core histone loci.

Overlapping binding sites for Spt10 and SBF in UAS3 and UAS4. Unlike UAS1 and UAS2, UAS3 and UAS4 contain overlapping high-affinity binding sites for Spt10 and SBF. The fact that nearly all of the critical bases in the Swi4 consensus site are also part of the downstream half-site recognized by Spt10 suggested that these proteins would be unable to bind simultaneously to the same UAS. However, the Swi4-DBD can bind at the same time as Spt10, presumably on the opposite face of the DNA helix, suggesting that the full-size proteins might perhaps bind simultaneously, if one or both were to undergo conformational changes. However, there was no sign of this *in vitro*, where Spt10 and SBF competed for binding to UAS3/UAS4.

Analysis of the sequences of the other major core histone gene promoters revealed only one exact match to the Swi4 consensus site, located near *HHF2*; this is a high-affinity site (D. J. Clark, unpublished data). Although this Swi4 site overlaps putative UAS6 (16), UAS6 is a weak match to the Spt10 consensus and does not bind Spt10 (G. Mendiratta, unpublished data). There are no high-affinity Swi4 sites in the *HTA2-HTB2* or the *HHT1-HHF1* promoters, but there are some weak sites that might have biological significance. Both the *HTZ1* and *HHO1* promoters contain a predicted high-affinity Swi4 site, suggesting that SBF also plays a significant role in the

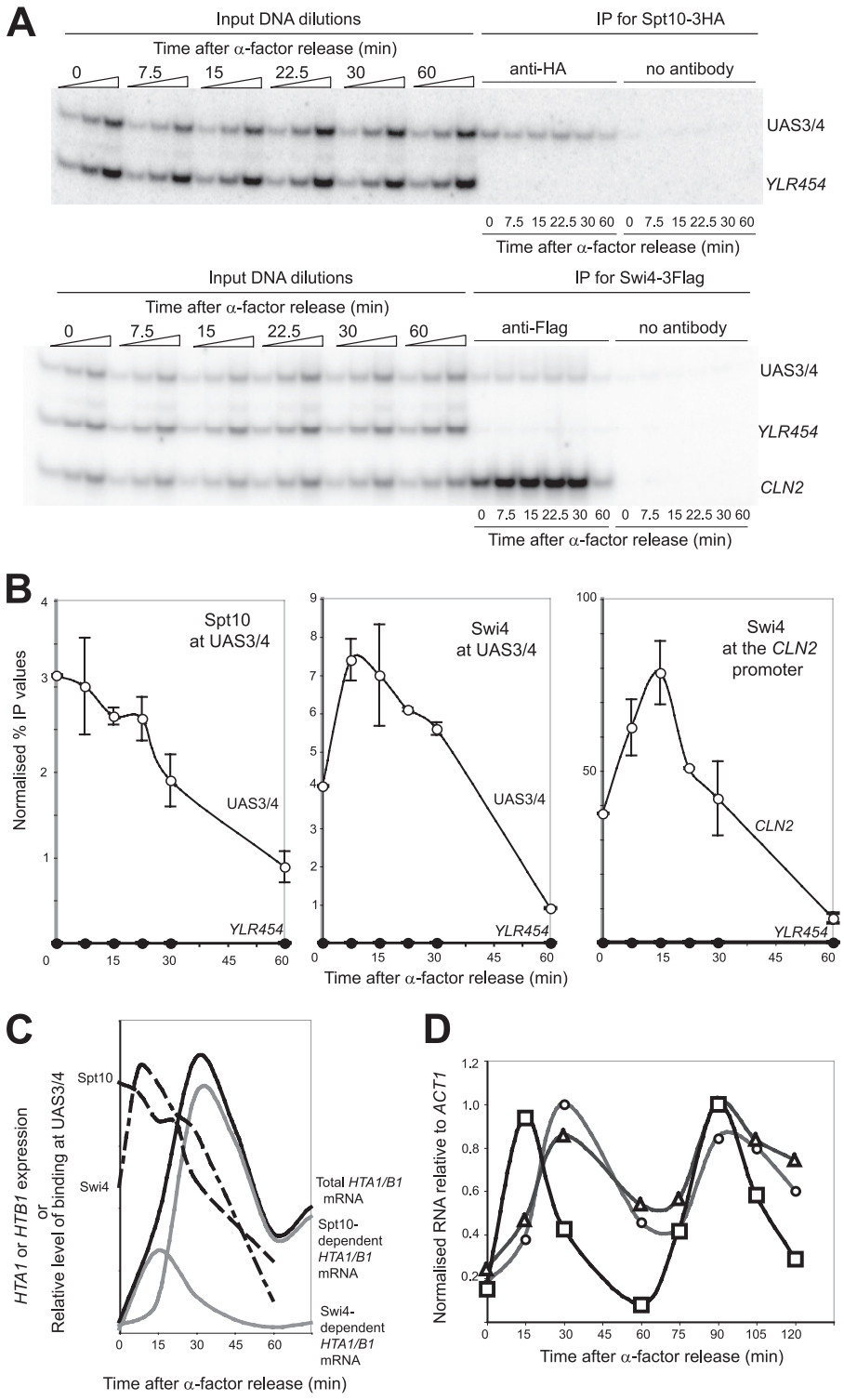

FIG. 7. The binding of Spt10 and Swi4 at the *HTA1-HTB1* promoter is cell cycle dependent. ChIP experiments used a yeast strain carrying *SPT10-3HA* and *SWI4-3Flag*. (A) Binding of Spt10 and Swi4 at the *HTA1-HTB1* promoter (phosphorimages). Multiplex PCR was done with primers for UAS3/UAS4, the coding region of *YLR454* (negative control), and the *CLN2* promoter (positive control for Swi4). The PCR products were 127 bp, 105 bp, and 82 bp, respectively. (B) Quantitation of Spt10 and Swi4 binding. Error bars indicate standard deviations for two independent experiments. The Swi4 data for the *CLN2* promoter are plotted separately because the signal was so strong. (C) Timing of Spt10 and Swi4 binding and *HTA1*/*HTB1* transcription (idealized). The relative amounts of Spt10 and Swi4 binding (dashed lines) should not be compared. The idealized expression of *HTA1* or *HTB1* is shown with the deduced contributions of Swi4 and Spt10 (gray lines) (see text). (D) Expression of *HTA1* (circles), *HTB1* (triangles), and *CLN2* (squares) over two cell cycles. Northern blot data were normalized to *ACT1* mRNA and to the highest value in each data set.

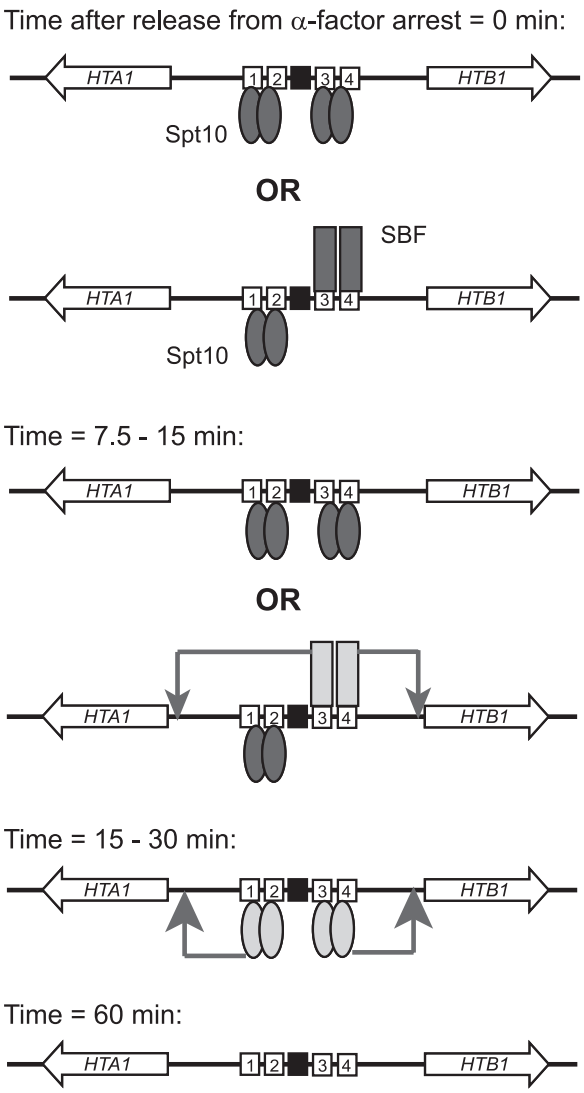

FIG. 8. Model for activation of *HTA1-HTB1*. At early times, there are at least two possible configurations for the *HTA1-HTB1* promoter, because the binding of SBF and Spt10 at UAS3/UAS4 is mutually exclusive (indicated by "OR"). Both Spt10 and SBF bind before *HTA1* and *HTB1* transcription is activated and are therefore inactive in arrested cells. SBF is activated first, driving small peaks of expression of both genes. Soon afterwards, Spt10 is activated, driving the major peaks of expression of both genes. After 60 min, little Swi4 is bound, and Spt10 is reduced to ~20% of its initial level. Numbered boxes, UASs; black box, NEG region; pair of ovals, Spt10 dimer; single rectangle, SBF. Inactive Spt10 and SBF are shaded dark; activated forms are shaded light. Arrows indicate activated promoters.

expression of H2A-Z and H1, respectively. Thus, overlapping Swi4 and Spt10 binding sites are not a general feature of histone gene regulation but appear to be specific for *HTA1-HTB1*, which is the most important of the two loci encoding H2A and H2B (45).

A working model for cell cycle-dependent activation of *HTA1-HTB1*. Based on our data and those of others, we propose a model for the activation of *HTA1-HTB1* (Fig. 8). In cells arrested with α-factor, Spt10 dimers may bind to UAS1/UAS2 and to UAS3/UAS4. There is competition between Spt10 and SBF for binding at UAS3/UAS4 but not at UAS1/UAS2. The relative occupancies of Spt10 and SBF at UAS3/UAS4 will be governed by their relative concentrations and affinities. Transcription factor binding to DNA is expected to be in dynamic equilibrium: each factor binds and dissociates, thus creating opportunities for competing factors to bind. The extent to which the UAS elements are assembled into nucleosomes will be important in determining which factors are bound and when they are bound.

In arrested cells, Spt10 and SBF bind but do not activate *HTA1-HTB1*. In the case of SBF, the lack of activation is due to Whi5, a repressor which binds to SBF at its target promoters in early G_1 phase (9, 10) and helps to recruit the histone deacetylase Rpd3L (62). This repression is later relieved by the phosphorylation of Whi5 by the Cln3-Cdc28 kinase (9, 10). SBF also directs the recruitment of the FACT complex (62). Nothing is known of this aspect of Spt10 regulation, but Spt10 activity might be regulated in an analogous manner, perhaps resulting in the activation of its putative HAT function, given that the HAT domain is capable of activating transcription *in vivo* (28). Alternatively, Spt10 might act at zero time, when its binding is maximal, leaving a memory of its presence (e.g., histone acetylation), which eventually facilitates transcription after 15 to 30 min.

Our model proposes that activated SBF stimulates *HTA1* and *HTB1* transcription, resulting in a small early peak of expression of both genes, ~7.5 min after α-factor removal. At this time, Spt10 remains inactive. After 15 to 30 min, Spt10 is activated and drives much larger peaks of expression of both genes. By ~30 min, Spt10 is fully active, but SBF contributes little. There is a precipitous decline in the binding of both Spt10 and SBF, which, in the case of SBF, reflects the phosphorylation of Swi6 and export from the nucleus (21). By 60 min, *HTA1* and *HTB1* are at their lowest point of expression, little or no SBF is bound, and the amount of bound Spt10 has declined to ~20% of its maximum. It is suggested that the remaining Spt10 returns to its inactive, poised state, awaiting the next S phase.

Roles of the UAS and NEG systems in the regulation of the histone genes. In the model (Fig. 8), it is implicit that the cell cycle regulation of *HTA1-HTB1* is centered on Spt10, SBF, and the UAS elements. However, there is strong evidence for an important role for the NEG region and its associated repressive factors in the cell cycle control of *HTA1-HTB1*: the deletion of NEG or of NEG-associated factors results in an altered cell cycle-dependent expression of *HTA1-HTB1* such that the level of expression remains high after the first peak, merging with the second (48, 50). Recently, it was proposed that the establishment of repressive chromatin domains is the primary mechanism of cell cycle regulation of the histone promoters (18). It was suggested that Rtt109 (the major HAT for H3-K56) together with the SWI/SNF and Yta7 chromatin-remodeling complexes counteract nucleosome assembly mediated by the histone chaperone Rtt106 and the HIR complex at the *HTA1-HTB1* promoter. In this model, the accessibility of the *HTA1-HTB1* promoter to RNA polymerase II is regulated through nucleosome assembly. However, no role for activators or the UAS elements was envisaged, even though *swi4*Δ and *spt10*Δ cells showed a reduced level of expression of an *HTA1*

reporter (18). Clearly, both systems play important roles in the regulation of *HTA1-HTB1*.

Instead, we propose that the primary mechanism of the cell cycle regulation of *HTA1-HTB1* is the UAS system operating through Spt10 and SBF. This is based on several lines of evidence. First, isolated UAS elements confer cell cycle-regulated expression on a reporter with the correct timing (20, 49). Although the CCR′ element, which is located within the NEG region, can also confer cell cycle regulation on a reporter, the timing is too early (49). Second, all four of the major histone gene promoters contain histone UAS elements, which bind Spt10 (16). Spt10 requires a pair of UAS elements to bind with high affinity, and these are not found anywhere else in the genome. Third, NEG elements have not been identified in *HTA2-HTB2* and so cannot account for the cell cycle regulation of this promoter. Fourth, Spt10 is not essential, but *spt10*Δ cells are very sick. Furthermore, the *spt10*Δ mutation is synthetically lethal with the *swi4*Δ mutation (29). This might well reflect the fact that both histone gene activators would be absent in the double mutant, although Swi4 is important for the activation of other genes at the G_1-to-S-phase transition. Finally, our data here show that multiple mutations in all four UAS elements in *HTA1-HTB1* almost completely eliminate reporter gene expression, even though the NEG region is intact.

Perhaps the most confusing aspect of the identification of Spt10 as the major activator of the histone genes has been that the levels of expression of three of the four histone loci are only modestly reduced in *spt10*Δ cells (*HTA2-HTB2* shows a stronger reduction in levels of expression than do the others) (16, 28). However, these measurements were performed with asynchronous cells; the loss of expression is much clearer in synchronized cells (68). The relatively mild effects on histone gene expression in *spt10*Δ cells can be accounted for by considering the following: (i) the defective chromatin structure assembled in the absence of Spt10 might result in a derepression of the basal transcription of the histone genes (16); (ii) the activation of *HTA1-HTB1* by a UAS belonging to another gene upstream or downstream of *HTA1-HTB1* might occur, since a UAS is effective at a much greater distance from its target gene in *spt10*Δ cells (13); (iii) the very slow growth of *spt10*Δ cells could reflect the existence of a checkpoint system requiring cells to wait until sufficient histone mRNA is produced to allow the completion of S phase; and (iv) the fact that the Spt10 half-site mutations eliminate all but the early, Swi4-dependent, peak of *HTA1* and *HTB1* expression is very good evidence that Spt10, working through the UAS elements, is indeed primarily responsible for the cell cycle-dependent expression of *HTA1-HTB1*. Because a reporter was used in this experiment, the effects of Spt10 on transcription are divorced from the indirect and downstream effects of aberrant histone gene expression.

So what might the role of the NEG system be? The NEG system might act as a checkpoint to communicate the presence of stalled replication forks to the histone genes. This hypothesis is based on the previously demonstrated role of NEG in shutting down histone gene expression in the presence of hydroxyurea (54, 58, 67). The NEG system might temporarily shut down the UAS system, awaiting a signal to continue, probably involving a chromatin-based mechanism (18). In other words, the NEG system modulates the activity of the UAS system. In this model, the fact that the CCR′ element (which is within the NEG region) confers cell cycle-dependent expression on a reporter driven by an unrelated UAS (49) could be accounted for by a repressor that recognizes CCR′, the activity of which is also under cell cycle control, such that it is inactive during early S phase. We are currently investigating this hypothesis.

ACKNOWLEDGMENTS

We thank Geetu Mendiratta for providing unpublished data. We thank Rohinton Kamakaka and David Stillman for helpful comments on the manuscript.

This work was supported by the Intramural Research Program of the NIH (NICHD).

REFERENCES

1. **Andrews, B. J., and L. A. Moore.** 1992. Interactions of the yeast Swi4 and Swi6 cell cycle regulatory proteins *in vitro*. Proc. Natl. Acad. Sci. U. S. A. **89:**11852–11856.
2. **Baetz, K., and B. Andrews.** 1999. Regulation of cell cycle transcription factor Swi4 through auto-inhibition of DNA binding. Mol. Cell. Biol. **19:**6729–6741.
3. **Bevis, B. J., and B. S. Glick.** 2002. Rapidly maturing variants of the *Discoma* red fluorescent protein (DsRed). Nat. Biotechnol. **20:**83–87.

3a. **Bradford, M. M.** 1976. A rapid and sensitive method for the quantitation of microgram quantities of protein utilizing the principle of protein-dye binding. Anal. Biochem. **72:**248–254.

4. **Breeden, L. L.** 2003. Periodic transcription: a cycle within a cycle. Curr. Biol. **13:**R31–R38.
5. **Breeden, L., and G. E. Mikesell.** 1991. Cell cycle-specific expression of the *SWI4* transcription factor is required for the cell cycle regulation of HO transcription. Genes Dev. **5:**1183–1190.
6. **Breeden, L., and K. Nasmyth.** 1987. Cell cycle control of the yeast *HO* gene: cis- and trans-activating regulators. Cell **48:**389–397.
7. **Campbell, S. G., M. del Olmo, P. Beglan, and U. Bond.** 2002. A sequence element downstream of the yeast *HTB1* gene contributes to mRNA 3′ processing and cell cycle regulation. Mol. Cell. Biol. **22:**8415–8425. (Author's correction, **28:**1873, 2008.)
8. **Clark-Adams, C. D., D. Norris, M. A. Osley, J. S. Fassler, and F. Winston.** 1988. Changes in histone gene dosage alter transcription in yeast. Genes Dev. **2:**150–159.
9. **Costanzo, M., et al.** 2004. CDK activity antagonizes Whi5, an inhibitor of G1/S transcription in yeast. Cell **117:**899–913.
10. **de Bruin, R. A. M., W. H. McDonald, T. I. Kalashnikova, J. Yates, and C. Wittenberg.** 2004. Cln3 activates G1-specific transcription via phosphorylation of the SBF-bound repressor Whi5. Cell **117:**887–898.
11. **Dimova, D., Z. Nackerdien, S. Furgeson, S. Eguchi, and M. A. Osley.** 1999. A role for transcriptional repressors in targeting the yeast SWI/SNF complex. Mol. Cell **4:**75–83.
12. **Dirick, L., T. Moll, H. Auer, and K. Nasmyth.** 1992. A central role for *SWI6* in modulating cell cycle Start-specific transcription in yeast. Nature **357:**507–513.
13. **Dobi, K. C., and F. Winston.** 2007. Analysis of transcriptional activation at a distance in *Saccharomyces cerevisiae*. Mol. Cell. Biol. **27:**5575–5586.
14. **Dollard, C., S. L. Ricupero-Hovasse, G. Natsoulis, J. D. Boeke, and F. Winston.** 1994. *SPT10* and *SPT21* are required for transcription of particular histone genes in *Saccharomyces cerevisiae*. Mol. Cell. Biol. **14:**5223–5228.
15. **Driscoll, R., A. Hudson, and S. P. Jackson.** 2007. Yeast Rtt109 promotes genome stability by acetylating histone H3 on lysine 56. Science **315:**649–652.
16. **Eriksson, P. R., et al.** 2005. Global regulation by the yeast Spt10 protein is mediated through chromatin structure and the histone upstream activating sequence elements. Mol. Cell. Biol. **25:**9127–9137.
17. **Fan, X., N. Lamarre-Vincent, Q. Wang, and K. Struhl.** 2008. Extensive chromatin fragmentation improves enrichment of protein binding sites in chromatin immunoprecipitation experiments. Nucleic Acids Res. **36:**e125.
18. **Fillingham, J., et al.** 2009. Two-color cell array screen reveals interdependent roles for histone chaperones and a chromatin boundary regulator in histone gene repression. Mol. Cell **35:**340–351.
19. **Formosa, T., et al.** 2002. Defects in *SPT16* or *POB3* (yFACT) in *Saccharomyces cerevisiae* cause dependence on the Hir/Hpc pathway: polymerase passage may degrade chromatin structure. Genetics **162:**1557–1571.
20. **Freeman, K. B., L. R. Karns, K. A. Lutz, and M. M. Smith.** 1992. Histone H3 transcription in *Saccharomyces cerevisiae* is controlled by multiple cell cycle activation sites and a constitutive negative regulatory element. Mol. Cell. Biol. **12:**5455–5463.
21. **Geymonat, M., A. Spanos, G. P. Wells, S. J. Smerdon, and S. G. Sedgwick.** 2004. Clb6/Cdc28 and Cdc14 regulate phosphorylation status and cellular localization of Swi6. Mol. Cell. Biol. **24:**2277–2285.

22. **Green, E. M., et al.** 2005. Replication-independent histone deposition by the HIR complex and Asf1. Curr. Biol. **15:**2044–2049.
23. **Groth, A., W. Rocha, A. Verreault, and G. Almouzni.** 2007. Chromatin challenges during DNA replication and repair. Cell **128:**721–733.
24. **Gunjan, A., J. Paik, and A. Verreault.** 2005. Regulation of histone synthesis and nucleosome assembly. Biochimie **87:**625–635.
25. **Han, J., et al.** 2007. Rtt109 acetylates histone H3 lysine 56 and functions in DNA replication. Science **315:**653–655.
26. **Harbison, C. T., et al.** 2004. Transcriptional regulatory code of a eukaryotic genome. Nature **431:**99–104.
27. **Hereford, L., K. Fahrner, J. Woolford, M. Rosbash, and D. B. Kaback.** 1979. Isolation of yeast histone genes H2A and H2B. Cell **18:**1261–1271.
28. **Hess, D., B. Liu, N. R. Roan, R. Sterglanz, and F. Winston.** 2004. Spt10-dependent transcriptional activation in *Saccharomyces cerevisiae* requires both the Spt10 histone acetyltransferase domain and Spt21. Mol. Cell. Biol. **24:**135–143.
29. **Hess, D., and F. Winston.** 2005. Evidence that Spt10 and Spt21 of *S. cerevisiae* play distinct roles in vivo and functionally interact with MCB-binding factor, SCB-binding factor and Snf1. Genetics **170:**87–94.
30. **Janke, C., et al.** 2004. A versatile toolbox for PCR-based tagging of yeast genes: new fluorescent proteins, more markers and promoter substitution cassettes. Yeast **21:**947–962.
31. **Kim, Y., and D. J. Clark.** 2002. SWI/SNF-dependent long-range remodeling of yeast *HIS3* chromatin. Proc. Natl. Acad. Sci. U. S. A. **99:**15381–15386.
32. **Kim, Y., N. McLaughlin, K. Lindstrom, T. Tsukiyama, and D. J. Clark.** 2006. Activation of *Saccharomyces cerevisiae HIS3* results in Gcn4p-dependent, SWI/SNF-dependent mobilization of nucleosomes over the entire gene. Mol. Cell. Biol. **26:**8607–8622.
33. **Koch, C., T. Moll, M. Neuberg, H. Ahorn, and K. Nasmyth.** 1993. A role for the transcription factors Mbp1 and Swi4 in progression from G1 to S-phase. Science **261:**1551–1557.
34. **Luger, K., A. W. Mader, R. K. Richmond, D. F. Sargent, and T. J. Richmond.** 1997. Crystal structure of the nucleosome core particle at 2.8 Å resolution. Nature **389:**251–260.
35. **Mariño-Ramirez, L., I. K. Jordan, and D. Landsman.** 2006. Multiple independent evolutionary solutions to core histone gene regulation. Genome Biol. **7:**R122.
36. **Mateus, C., and S. V. Avery.** 2000. Destabilized green fluorescent protein for monitoring dynamic changes in yeast gene expression with flow cytometry. Yeast **16:**1313–1323.
37. **Mellor, J.** 2009. Linking the cell cycle to histone modifications: Dot1, G1/S and cycling K79me2. Mol. Cell **35:**729–730.
38. **Mendiratta, G., P. R. Eriksson, C. H. Shen, and D. J. Clark.** 2006. The DNA-binding domain of the yeast Spt10p activator includes a zinc finger that is homologous to foamy virus integrase. J. Biol. Chem. **281:**7040–7048.
39. **Mendiratta, G., P. R. Eriksson, and D. J. Clark.** 2007. Cooperative binding of the yeast Spt10 activator to the histone upstream activating sequences is mediated through an N-terminal dimerization domain. Nucleic Acids Res. **35:**812–821.
40. **Moran, L., D. Norris, and M. A. Osley.** 1990. A yeast H2A-H2B promoter can be regulated by changes in histone gene copy number. Genes Dev. **4:**752–763.
41. **Natsoulis, G., C. Dollard, F. Winston, and J. D. Boeke.** 1991. The products of the *SPT10* and *SPT21* genes of *Saccharomyces cerevisiae* increase the amplitude of transcriptional regulation at a large number of unlinked loci. New Biol. **3:**1249–1259.
42. **Natsoulis, G., F. Winston, and J. D. Boeke.** 1994. The *SPT10* and *SPT21* genes of *Saccharomyces cerevisiae*. Genetics **136:**93–105.
43. **Neuwald, A. F., and D. Landsman.** 1997. *GCN5*-related histone N-acetyltransferases belong to a diverse superfamily that includes the yeast *SPT10* protein. Trends Biochem. Sci. **22:**154–155.
44. **Ng, H. H., F. Robert, R. A. Young, and K. Struhl.** 2002. Genome-wide location and regulated recruitment of the RSC nucleosome-remodeling complex. Genes Dev. **16:**806–819.
45. **Norris, D., and M. A. Osley.** 1987. The two gene pairs encoding H2A and H2B play different roles in the *Saccharomyces cerevisiae* life cycle. Mol. Cell. Biol. **7:**3473–3481.
46. **Nourani, A., F. Robert, and F. Winston.** 2006. Evidence that Spt2/Sin1, an HMG-like factor, plays roles in transcription elongation, chromatin structure and genome stability in *Saccharomyces cerevisiae*. Mol. Cell. Biol. **26:**1496–1509.
47. **Ogas, J., B. J. Andrews, and I. Herskowitz.** 1991. Transcriptional activation of *CLN1*, *CLN2* and a putative new G1 cyclin (*HCS26*) by SWI4, a positive regulator of G1-specific transcription. Cell **66:**1015–1026.
48. **Osley, M. A.** 1991. The regulation of histone synthesis in the cell cycle. Annu. Rev. Biochem. **60:**827–861.
49. **Osley, M. A., J. Gould, S. Kim, M. Kane, and L. Hereford.** 1986. Identification of sequences in a yeast histone promoter involved in periodic transcription. Cell **45:**537–545.
50. **Osley, M. A., and D. Lycan.** 1987. Trans-acting regulatory mutations that alter transcription of *Saccharomyces cerevisiae* histone genes. Mol. Cell. Biol. **7:**4204–4210.
51. **Prochasson, P., L. Florens, S. K. Swanson, M. P. Washburn, and J. L. Workman.** 2005. The HIR corepressor complex binds to nucleosomes generating a distinct protein/DNA complex resistant to remodeling by SWI/SNF. Genes Dev. **19:**2534–2539.
52. **Schulze, J. M., et al.** 2009. Linking cell cycle to histone modifications: SBF and H2B mono-ubiquitination machinery and cell-cycle regulation of H3K79 dimethylation. Mol. Cell **35:**626–641.
53. **Sharp, J. A., E. T. Fouts, D. C. Krawitz, and P. D. Kaufman.** 2001. Yeast histone deposition protein Asf1p requires Hir proteins and PCNA for heterochromatic silencing. Curr. Biol. **11:**463–473.
54. **Sherwood, P. W., and M. A. Osley.** 1991. Histone regulatory (*hir*) mutations suppress δ insertion alleles in *Saccharomyces cerevisiae*. Genetics **128:**729–738.
55. **Sidorova, J. M., G. E. Mikesell, and L. L. Breeden.** 1995. Cell cycle-regulated phosphorylation of Swi6 controls its nuclear regulation. Mol. Biol. Cell **6:**1641–1658.
56. **Simon, L., et al.** 2001. Serial regulation of transcriptional regulators in the yeast cell cycle. Cell **106:**697–708.
57. **Smith, M. M., and K. Murray.** 1983. Yeast H3 and H4 histone messenger RNAs are transcribed from two non-allelic gene sets. J. Mol. Biol. **169:**641–661.
58. **Spector, M. S., A. Raff, H. DeSilva, K. Lee, and M. A. Osley.** 1997. Hir1p and Hir2p function as transcriptional co-repressors to regulate histone gene transcription in the *Saccharomyces cerevisiae* cell cycle. Mol. Cell. Biol. **17:**545–552.
59. **Sutton, A., J. Bucaria, M. A. Osley, and R. Sternglanz.** 2001. Yeast ASF1 protein is required for cell cycle regulation of histone gene transcription. Genetics **158:**587–596.
60. **Taba, M. R., I. Muroff, D. Lydall, G. Tebb, and K. Nasmyth.** 1991. Changes in a SWI4/6 DNA-binding complex occur at the time of HO gene activation in yeast. Genes Dev. **5:**2000–2013.
61. **Tagami, H., D. Ray-Gallet, G. Almouzni, and Y. Nakatani.** 2004. Histone H3.1 and H3.3 complexes mediate nucleosome assembly pathways dependent or independent of DNA synthesis. Cell **116:**51–61.
62. **Takahata, S., Y. Yu, and D. J. Stillman.** 2009. The E2F functional analogue SBF recruits the Rpd3(L) HDAC, via Whi5 and Stb1, and the FACT chromatin reorganizer, to yeast G1 cyclin promoters. EMBO J. **28:**3378–3389.
63. **Taylor, I. A., et al.** 2000. Characterization of the DNA-binding domains from the yeast cell-cycle transcription factors Mbp1 and Swi4. Biochemistry **39:**3943–3954.
64. **Wach, A.** 1996. PCR-synthesis of marker cassettes with long flanking homology regions for gene disruptions in *S. cerevisiae*. Yeast **12:**259–265.
65. **Wang, G. G., C. D. Allis, and P. Chi.** 2007. Chromatin remodeling and cancer, part I: covalent histone modifications. Trends Mol. Med. **13:**363–372.
66. **Xu, H., L. Johnson, and M. Grunstein.** 1990. Coding and noncoding sequences at the 3′ end of yeast histone H2B mRNA confer cell cycle regulation. Mol. Cell. Biol. **10:**2687–2694.
67. **Xu, H., U. Kim, T. Schuster, and M. Grunstein.** 1992. Identification of a new set of cell cycle-regulatory genes that regulate S-phase transcription of histone genes in *Saccharomyces cerevisiae*. Mol. Cell. Biol. **12:**5249–5259.
68. **Xu, F., K. Zhang, and M. Grunstein.** 2005. Acetylation in histone H3 globular domain regulates gene expression in yeast. Cell **121:**375–385.